Energy flux in viscoelastic anisotropic media

Vlastislav Červený [1)], Ivan Pšenčík [2)]

1) Department of Geophysics, Faculty of Mathematics and Physics, Charles University, KB Karlovu 3, 121 16 Praha 2, Czech Republic. E-mail vcerveny@seis.karlov.mff.cuni.cz
2) Geophysical Institute, Acad. Sci. of Czech Republic, Boční II, 141 31 Praha 4, Czech Republic. E-mail ip@ig.cas.cz

Summary

Properties of the complex-valued Poynting vector **F** of homogeneous and inhomogeneous time-harmonic plane waves, propagating in an unbounded viscoelastic anisotropic medium are investigated, both analytically and numerically. The real-valued part of the Poynting vector represents the time-averaged energy flux, and its imaginary-valued part is closely related to the dissipated energy D_{diss}. An algorithm for the computation of the Poynting vector is proposed, which can be used for media of unrestricted anisotropy and viscoelasticity, and for arbitrary homogeneous or inhomogeneous plane waves. Numerical examples are presented, illustrating behaviour of the Poynting vector and other energy quantities, for homogeneous/inhomogeneous plane P, SV and SH waves.

Keywords
Viscoelastic anisotropic media, inhomogeneous plane waves, Poynting vector, time-averaged energy flux, attenuation vector.

1 Introduction

In this paper, we study the properties of energy flux of homogeneous and inhomogeneous time-harmonic plane waves propagating in an unbounded viscoelastic anisotropic medium. The complex-valued Poynting vector **F** (also called Umov-Poynting vector) is used as the quantity which fully characterizes the energy flux and the dissipation of energy of the wave. The real part of the Poynting vector represents the density of the time-averaged energy flux **S**, and its imaginary part is closely related to the density of the time-averaged dissipated energy D_{diss}: D_{diss} equals twice the magnitude of the projection of Im**F** to the propagation vector **P** (real part of the slowness vector, perpendicular to the wavefront). The aim of this paper is to present a concise derivation of the expression for the Poynting vector of homogeneous and inhomogeneous plane waves propagating in an unbounded medium of unrestricted anisotropy and viscoelasticity, to propose an algorithm for its calculation,

---

Seismic Waves in Complex 3-D Structures, Report 15 (Department of Geophysics, Charles University, Prague 2005), pp.295-332

and to perform analytical and numerical studies necessary for correct understanding of energy propagation and dissipation of relevant plane waves.

Considerable attention in seismology has been devoted to the energy flux of plane waves propagating in elastic anisotropic and in viscoelastic isotropic media. For elastic anisotropic media, see, for example, Fedorov (1968), Auld (1973), Burridge (1976), Gajewski and Pšenčík (1991), Helbig (1994), Carcione (2001), Červený (2001a), where many other references can be found. Energy flux of inhomogeneous plane waves in elastic anisotropic media was discussed by Hayes (1980) and Deschamps and Poncelet (2002). For viscoelastic isotropic media, see Buchen (1971), Borcherdt (1973), Aki and Richards (1980), Krebes (1983), Richards (1984), Borcherdt and Wennerberg (1985), Mann et al. (1987), Leroy et al. (1988), Deschamps (1990), Caviglia and Morro (1992, 1999), Ainslie and Burns (1995), Brokešová and Červený (1998), Carcione (2001). In many parts of the Earth's interior, however, both anisotropy and viscoelasticity appear together and thus viscoelastic anisotropic media must be considered. Certain useful relations for energy flux of plane waves in viscoelastic anisotropic media can be already found in the classical book by Auld (1973). The book, however, considers mostly homogeneous plane waves. Systematic study of both homogeneous and inhomogeneous plane waves in viscoelastic anisotropic media can be found in a series of papers by Carcione, see Carcione (1994, 1995, 1997a,b, 2001), and Carcione and Cavallini (1993, 1995). See also Krebes and Le (1994), Červený (2001b). An excellent treatment of the Poynting vector, dissipated energy, and related energy quantities can be found particularly in the paper by Carcione and Cavallini (1993). Certain equations presented here have been derived already in that paper. For viscoporoelastic anisotropic media, see the pioneering papers by Hanyga (1999) and by Hanyga and Seredyńska (1999).

The algorithms of the computation of the Poynting vector in viscoelastic anisotropic media depend on the complexity of anisotropy in the medium. For SH homogeneous and inhomogeneous plane waves propagating in a plane of symmetry of a monoclinic (orthorhombic, hexagonal) viscoelastic medium, analytical solutions can be found. See Krebes and Le (1994), and Carcione and Cavallini (1995), where certain interesting properties of energy flux in viscoelastic anisotropic media were described. The general algorithms for unrestricted anisotropy and viscoelasticity, however, have been proposed only recently. The basic role in these algorithms is played by the method of determination of the complex-valued slowness vector $\mathbf{p} = \mathbf{P} + \mathrm{i}\mathbf{A}$, satisfying equation of motion. Several alternative, but mutually related, methods have been proposed to compute $\mathbf{p}$. For a detailed description of these methods see Červený and Pšenčík (2005a). One of them is based on the generalization of the so-called Stroh formalism for viscoelastic media. It was used by Caviglia and Morro (1999) to discuss theoretically the reflection/transmission of plane waves at a plane interface between two viscoelastic anisotropic media. A great attention in that paper was also devoted to the theoretical treatment of Poynting vector. The Stroh formalism has been also applied to studying theoretically homogeneous and inhomogeneous plane waves in perfectly elastic, viscoelastic and thermoviscoelastic anisotropic media, including the energy flux, by Shuvalov and Scott (1999, 2000), and Shuvalov (2001). A method close to the Stroh formalism has been also used traditionally in seismology for perfectly elastic media to compute the velocity-stress propagators in one-dimensional anisotropic structures, see Frazer and Fryer (1989), Thomson (1996a,b), etc. This theory can be also generalized for viscoelastic anisotropic media, as shown in

the presented references. Here we shall use the method proposed in Červený (2004) and Červený and Pšenčík (2005a), based on the so-called mixed specification of the slowness vector, see Section 3.1. In the mixed specification, the slowness vector is expressed in terms of a complex-valued constant σ, which can be determined as a root of an algebraic equation of the sixth degree. The algebraic equation for σ is supplemented by a system of linear equations for the determination of the amplitude vectors $\mathbf{U}$. These quantities are sufficient to determine the Poynting vector $\mathbf{F}$ and all related energy quantities. A more detailed description and comparison of individual approaches can be found in Červený and Pšenčík (2005a).

With the exception of papers by Krebes and Le (1994) and Carcione and Cavallini (1995), in which the SH plane waves in a symmetry plane of an anisotropic viscoelastic medium were studied, the authors do not know any paper in which the energy flux and other related energy quantities of homogeneous and inhomogeneous plane waves propagating in a viscoelastic anisotropic medium would be numerically studied. Particularly, numerical studies for P and SV waves are not available.

In Section 2, energy balance equations for time-harmonic waves propagating in an inhomogeneous viscoelastic anisotropic medium are derived. Important energy quantities, as the complex-valued Poynting vector $\mathbf{F}$, real-valued time-averaged kinetic energy K, strain energy U, complete energy $E = K + U$, and dissipated energy D_{diss}, are introduced. Moreover, the time-averaged energy flux $\mathbf{S}$ is introduced as the real part of $\mathbf{F}$, and the energy velocity vector as $\boldsymbol{\mathcal{U}} = \mathbf{S}/E$. Actually, these quantities represent the densities of the relevant quantities, but the word "density" is mostly omitted in this paper.

In Section 3, all energy quantities are specified for time-harmonic, homogeneous and inhomogeneous plane waves. In Section 3.1, the algorithms for the computation of the complex-valued slowness vector $\mathbf{p}$ and for complex-valued amplitude vector $\mathbf{U}$ are explained. Section 3.2 presents equations for the Poynting vector $\mathbf{F}$ and for other energy quantities, for homogeneous and inhomogeneous plane waves. Various relations between the energy quantities and the propagation vector $\mathbf{P}$ and attenuation vector $\mathbf{A}$ are derived and discussed.

In Section 4, the significant directions of plane waves propagating in viscoelastic anisotropic media, and the angles between the real and imaginary parts of certain complex-valued vectors, are studied. All the equations presented in Sections 2, 3 and 4 are valid quite generally, for inhomogeneous and homogeneous P, S1 and S2 plane waves, propagating in media with unrestricted anisotropy and viscoelasticity.

In Section 5, SH plane waves, propagating in a plane of symmetry of monoclinic (orthorhombic, hexagonal) anisotropic viscoelastic media, are studied. In this case, the algebraic equation of the sixth degree reduces to quadratic equation. Consequently, all equations for the Poynting vector and other energy quantities may be expressed analytically in this case. These analytical solutions offer a simple physical insight into the energy flux quantities in anisotropic viscoelastic media, and into their properties and mutual relations. Analytical procedures of Section 5 are supplemented by numerical examples in Section 6. Finally, the properties of Poynting vector and of other energy quantities of homogeneous and inhomogeneous plane P and S waves are investigated numerically in Section 7.

We use Cartesian coordinates x_i, and denote the time t, the Cartesian components of the displacement vector $u_i(x_k,t)$, of the particle velocity $v_i(x_k,t) = \dot{u}_i(x_k,t)$, of the stress tensor $\tau_{ij}(x_k,t)$, and of the infinitesimal strain tensor $e_{ij}(x_l,t)$. Both tensors τ_{ij} and e_{ij} are symmetric, $\tau_{ij} = \tau_{ji}$ and $e_{ij} = e_{ji}$. The infinitesimal strain tensor e_{ij} is expressed in terms of the displacement vector as follows:

$$e_{ij} = \tfrac{1}{2}(u_{i,j} + u_{j,i}) \ . \tag{1}$$

The dot above the letter denotes the partial derivative with respect to time ($\dot{v}_i = \partial v_i/\partial t$), the index behind the comma in the subscript indicates the partial derivative with respect to the relevant Cartesian coordinate ($u_{i,j} = \partial u_i/\partial x_j$). The Einstein summation convention over repeating indices is used throughout the paper.

2 Energy balance equations for time-harmonic waves

We consider wavefield in an inhomogeneous viscoelastic anisotropic media, satisfying the equation of motion,

$$\tau_{ij,j} + f_i = \rho \dot{v}_i \ , \tag{2}$$

where $\rho = \rho(x_k)$ is the density, and $f_i(x_l,t)$ are Cartesian components of the body force vector $\mathbf{f}(x_l,t)$ (force per unit volume).

For time-harmonic wave fields, we consider the exponential time factor $\exp[-\mathrm{i}\omega t]$, where ω is a fixed positive circular frequency, $\omega > 0$. The generalized Hooke's law for viscoelastic anisotropic solid can be simply derived from the Hooke's law for perfectly elastic media using the correspondence principle, see Carcione (2001, p. 102). It is sufficient to substitute elastic moduli in the standard Hooke's law by viscoelastic ones. The generalized Hooke's law then reads

$$\tau_{ij} = c_{ijkl} e_{kl} \ , \tag{3}$$

where $c_{ijkl}(x_n,\omega)$ are complex-valued frequency-dependent viscoelastic moduli. As ω is fixed, we do not explicitly indicate the frequency-dependence of c_{ijkl}. The viscoelastic moduli c_{ijkl} satisfy the symmetry relations:

$$c_{ijkl} = c_{jikl} = c_{ijlk} = c_{klij} \ , \tag{4}$$

so that the number of independent viscoelastic moduli reduces from 81 to 21. Alternatively to the viscoelastic moduli c_{ijkl}, we also use the density-normalized viscoelastic moduli $a_{ijkl} = c_{ijkl}/\rho$. The density-normalized viscoelastic moduli also satisfy the symmetry relations (4).

Often, the Voigt notation has been used for τ_{ij}, e_{kl} and c_{ijkl}, in which two indices i,j ($i,j = 1,2,3$) are replaced by one index α ($\alpha = 1,2,...,6$), and similarly two indices k,l ($k,l = 1,2,3$) by one index β ($\beta = 1,2,...,6$). Then (3) can be expressed in the form $\tau_\alpha = C_{\alpha\beta} e_\beta$, where $C_{\alpha\beta}$ represents a 6×6 symmetric matrix. The symmetry relations (4) reduce to one symmetry relation $C_{\alpha\beta} = C_{\beta\alpha}$ in this case. See Fedorov (1968), Auld (1973), Carcione (1994, 1995, 1997a,b, 2001), and Carcione and Cavallini (1993, 1995).

Analogously to $C_{\alpha\beta}$, we also introduce the Voigt notation $A_{\alpha\beta}$ for the density-normalized viscoelastic moduli.

We shall now derive the energy balance equations for time-harmonic waves, propagating in inhomogeneous anisotropic media. See also Auld (1973), Carcione and Cavallini (1993), and Carcione (2001).

Multiplying (2) by $-v_i^*$, and the complex-conjugate of the time-derivative of (1) by $-\tau_{ij}$, and adding both, we obtain

$$(-v_i^*\tau_{ij})_{,j} = -\rho v_i^*\dot{v}_i - \tau_{ij}\dot{e}_{ij}^* + v_i^* f_i \ . \tag{5}$$

For time-harmonic waves, with the exponential time factor $\exp[-\mathrm{i}\omega t]$, (5) yields,

$$(-v_i^*\tau_{ij})_{,j} = \mathrm{i}\omega\rho(v_i v_i^* - \tau_{ij}e_{ij}^*) + v_i^* f_i \ . \tag{6}$$

Equations (5) and (6) are exact, valid for elastic and viscoelastic, isotropic and anisotropic, media. It is common to express (6) in the following form

$$\mathrm{div}\mathbf{F} = 2\mathrm{i}\omega(K - U) - \omega D + P \ , \tag{7}$$

where

$$\begin{array}{ll} K = \frac{1}{4}\rho v_i v_i^* \ , & U = \frac{1}{4}\mathrm{Re}(\tau_{ij}e_{ij}^*) \ , \\ D_{diss} = -\frac{1}{2}\mathrm{Im}(\tau_{ij}e_{ij}^*) \ , & P = \frac{1}{2}f_i v_i^* \ , \\ F_j = -\frac{1}{2}v_i^*\tau_{ij} \ . & \end{array} \tag{8}$$

Equation (7) is called the energy balance equation for time-harmonic waves for inhomogeneous anisotropic viscoelastic medium. Note that K, U and D_{diss} are real-valued scalars, P is a complex-valued scalar, and $\mathbf{F}$ the complex-valued vector.

Individual terms in (7) are usually interpreted as follows, see, for example Auld (1973), and Carcione and Cavallini (1993): K and U are time-averaged kinetic and strain energies, respectively, D_{diss} is the time-averaged dissipated energy, P is the time-averaged energy supplied by body forces (per unit volume), and $\mathbf{F}$ is the time-averaged complex-valued energy flux vector. We also introduce the real-valued time-averaged complete energy E by the relation

$$E = U + K \ . \tag{9}$$

The time-averaging is understood for one period $T = 2\pi/\omega$.

The complex-valued energy flux vector $\mathbf{F}$ is also called Poynting vector, or the Umov-Poynting vector. The real part of the Poynting vector $\mathbf{F}$ represents the time-averaged energy flux vector $\mathbf{S}$,

$$\mathbf{S} = \mathrm{Re}(\mathbf{F}) \ . \tag{10}$$

Using $\mathbf{S}$, we can introduce an important concept of time-averaged energy velocity vector $\boldsymbol{\mathcal{U}}$

$$\boldsymbol{\mathcal{U}} = \mathbf{S}/E \ . \tag{11}$$

The introduced quantities are measured in the following units: stress τ_{ij}, the elastic moduli c_{ijkl} and $C_{\alpha\beta}$ and the energy quantities U, K, E and D in pascals (Pa; $\mathrm{kg\,m^{-1}s^{-2}}$), the components of body forces f_i in Newton per cubic meter ($\mathrm{N/m^3}$; $\mathrm{kg\,m^{-2}s^{-2}}$), density

ρ in kilograms per cubic meter ($\mathrm{kg\,m^{-3}}$), displacement components u_i in meters (m), the velocity components v_i in $\mathrm{m\,s^{-1}}$, the density-normalized elastic moduli a_{ijkl} and $A_{\alpha\beta}$ in $\mathrm{m^2 s^{-2}}$, the quantity P in pascals per second ($\mathrm{Pa\,s^{-1}}$; $\mathrm{kg\,m^{-1}s^{-3}}$), the Poynting vector $\mathbf{F}$ in watt per square meter ($\mathrm{W\,m^{-2}}$; $\mathrm{kg\,s^{-3}}$), and the energy velocity vector $\boldsymbol{\mathcal{U}}$ in $\mathrm{m\,s^{-1}}$.

Whereas the Poynting vector $\mathbf{F}$ is, by definition, a complex-valued vector, the time-averaged energy flux vector $\mathbf{S}$ and the energy velocity vector $\boldsymbol{\mathcal{U}}$ are real-valued vectors.

We can insert the generalized Hooke's law (3) into (8). The expressions for U, D_{diss} and F_j are then as follows:

$$\begin{aligned} U &= \tfrac{1}{4}\mathrm{Re}(c_{ijkl}e_{kl}e^*_{ij}) \ , \quad D_{diss} = -\tfrac{1}{2}\mathrm{Im}(c_{ijkl}e_{kl}e^*_{ij}) \ . \\ F_j &= -\tfrac{1}{2}v^*_i c_{ijkl}e_{kl} \ . \end{aligned} \tag{12}$$

We prove that U is positive if $\mathrm{Re}(c_{ijkl})$ is positive definite, and D_{diss} non-negative for $\mathrm{Im}(c_{ijkl})$ negative definite or zero, with respect to the pairs of indices i,j and k,l. Using the Voigt notation, we obtain

$$c_{ijkl}e_{kl}e^*_{ij} = C_{\alpha\beta}e^*_\alpha e_\beta = C_{\alpha\beta}(e^R_\alpha e^R_\beta + e^I_\alpha e^I_\beta) \ ,$$

where $e^R_\alpha = \mathrm{Re}(e_\alpha)$, $e^I_\alpha = \mathrm{Im}(e_\alpha)$, and similarly for e_β. The quantities e^R_α and e^I_α represent real-valued components of 6×1 real-valued vectors ($\alpha,\beta = 1,2,...,6$). Since strain energy must be positive, $U>0$, it implies that $\mathrm{Re}C_{\alpha\beta}$ must be positive definite. Similarly, since D_{diss} must be positive or equal zero, $-\mathrm{Im}C_{\alpha\beta}$ must be positive definite or zero.

3 Energy flux of a plane wave

We consider a homogeneous unbounded viscoelastic anisotropic medium, and a time-harmonic plane wave, propagating in the medium,

$$u_i(x_j,t) = U_i \exp[-\mathrm{i}\omega(t - p_n x_n)] \ . \tag{13}$$

Here $\mathbf{p}$ is a complex-valued slowness vector, and $\mathbf{U}$ a complex-valued amplitude vector. Equation (13) represents a plane wave only if $\mathbf{U}$ and $\mathbf{p}$ are chosen in such a way that (13) satisfies the equation of motion, see (2) and (3). This requirement yields a system of linear equations for U_1, U_2, U_3:

$$a_{ijkl}p_j p_l U_k = U_i \ , \quad i = 1,2,3 \ . \tag{14}$$

The condition of solvability of system (14),

$$\det[a_{ijkl}p_j p_l - \delta_{ik}] = 0 \ , \tag{15}$$

is the constraint relation for the slowness vector $\mathbf{p}$. Eq. (14) is the constraint relation for the amplitude vector $\mathbf{U}$. The polarization vector $\mathbf{U}$ may be, of course, suitably normalized.

3.1 Determination of slowness vectors

The determination of the slowness vector $\mathbf{p}$ which satisfies the constraint relation (15) is not straightforward. To do it, it is useful to specify the slowness vector in the following way,

$$\mathbf{p} = \sigma\mathbf{n} + \mathrm{i}D\mathbf{m} \ , \qquad \text{with} \ \ \mathbf{m}\cdot\mathbf{n} = 0 \ . \tag{16}$$

Here $\mathbf{n}$ and $\mathbf{m}$ are two arbitrary, mutually perpendicular real-valued unit vectors; they are perpendicular and tangent to the wavefront Σ, respectively. The quantity D is a scalar real-valued quantity called inhomogeneity parameter, $D \in (-\infty, \infty)$. The unit vectors $\mathbf{n}$, $\mathbf{m}$ and the inhomogeneity parameter D can be arbitrarily chosen, and the complex-valued quantity σ is then determined from

$$\det[a_{ijkl}(\sigma n_j + \mathrm{i}Dm_j)(\sigma n_l + \mathrm{i}Dm_l) - \delta_{ik}] = 0 \ , \tag{17}$$

which results from (15). This is an algebraic equation of the sixth degree for σ. It has six complex-valued roots σ, corresponding to P, S1 and S2 waves, propagating in opposite directions from Σ.

Once the quantity σ has been found, we can simply determine the complex-valued slowness vector,

$$\mathbf{p} = \mathbf{P} + \mathrm{i}\mathbf{A} \ , \tag{18}$$

so that

$$\mathbf{P} = \mathbf{n}\,\mathrm{Re}\sigma \ , \qquad \mathbf{A} = \mathbf{n}\,\mathrm{Im}\sigma + D\mathbf{m} \ . \tag{19}$$

Here $\mathbf{P}$ is called the propagation vector. It is perpendicular to the wavefront Σ, and oriented in the direction of the propagation of the wavefront. The vector $\mathbf{A}$ is called the attenuation vector, perpendicular to the plane of constant amplitude, oriented in the direction of the maximum decay of amplitudes. We can further compute the lengths of vectors $\mathbf{P}$ and $\mathbf{A}$, $|\mathbf{P}|$ and $|\mathbf{A}|$, the unit vectors $\mathbf{N}$ and $\mathbf{M}$ along $\mathbf{P}$ and $\mathbf{A}$, phase velocity $\mathcal{C}$ and the attenuation angle γ ($\cos\gamma = \mathbf{N}\cdot\mathbf{M}$):

$$\begin{array}{ll} |\mathbf{P}| = |\mathrm{Re}\sigma| \ , & |\mathbf{A}| = [(\mathrm{Im}\sigma)^2 + D^2]^{1/2} \ , \\ \mathbf{N} = \mathbf{P}/|\mathbf{P}| = \epsilon\mathbf{n} \ , & \mathbf{M} = \mathbf{A}/|\mathbf{A}| \ , \\ \mathcal{C} = 1/|\mathrm{Re}\sigma| \ , & \cos\gamma = \epsilon(\mathrm{Im}\sigma)/[(\mathrm{Im}\sigma)^2 + D^2]^{1/2} \ , \end{array} \tag{20}$$

where $\epsilon = \mathrm{Re}\sigma/|\mathrm{Re}\sigma| = \pm 1$. For more details see Červený and Pšenčík (2005a).

Note that the plane wave with real-valued slowness vector $\mathbf{p}$ ($\mathbf{A} = \mathbf{0}$) is called here the bulk plane wave, the plane wave with $\mathbf{A} \neq \mathbf{0}$ and $D = 0$ the homogeneous plane wave, and the plane wave with $\mathbf{A} \neq \mathbf{0}$ and $D \neq 0$ the inhomogeneous plane wave. For homogeneous plane waves, $\mathbf{P}$ and $\mathbf{A}$ are parallel, and for inhomogeneous plane waves, they are not. The plane specified by $\mathbf{P}$ and $\mathbf{A}$ (or by $\mathbf{n}$ and $\mathbf{m}$) is called the propagation-attenuation plane $\Sigma^{\parallel}$.

3.2 Poynting vector

Once the plane wave (13), including $\mathbf{p}$ and $\mathbf{U}$, has been determined, we can find an explicit equation for the complex-valued Poynting vector $\mathbf{F}$ from (8). For $\dot{u}_i$ and τ_{ij}, we obtain

$$\dot{u}_i \ = \ -\mathrm{i}\omega U_i \exp[-\mathrm{i}\omega(t - p_n x_n)] \ ,$$

$$\tau_{ij} \;=\; \mathrm{i}\omega\rho a_{ijkl}U_l p_k \exp[-\mathrm{i}\omega(t - p_n x_n)] \; .$$

Poynting vector $\mathbf{F}$ then reads

$$F_i = \tfrac{1}{2}\rho\omega^2 a_{ijkl}U_j^* U_l p_k \exp[-2\omega A_n x_n] \; . \tag{21}$$

Here p_l must satisfy (15), and U_k (14).

The time-averaged energy flux $\mathbf{S}$ is then given by the equation:

$$S_i = \mathrm{Re}(F_i) = \tfrac{1}{2}\rho\omega^2 \mathrm{Re}(a_{ijkl}U_k U_j^* p_l) \exp[-2\omega A_n x_n] \; . \tag{22}$$

Analogously, we obtain explicit expressions for other important energy quantities: the time-averaged kinetic energy K, time-averaged strain energy U, and the time-averaged dissipated energy D_{diss}, see (8):

$$\begin{aligned} K &= \tfrac{1}{4}\rho\omega^2 U_i U_i^* \exp[-2\omega A_n x_n] \; , \\ U &= \tfrac{1}{4}\rho\omega^2 \mathrm{Re}(a_{ijkl}U_k U_i^* p_l p_j^*) \exp[-2\omega A_n x_n] \; , \\ D_{diss} &= -\tfrac{1}{2}\rho\omega^2 \mathrm{Im}(a_{ijkl}U_k U_i^* p_l p_j^*) \exp[-2\omega A_n x_n] \; . \end{aligned} \tag{23}$$

From (11), we get the expression for the time-averaged energy velocity vector $\boldsymbol{\mathcal{U}}$:

$$\mathcal{U}_i = \frac{S_i}{E} = \frac{2\mathrm{Re}(a_{ijkl}U_k U_j^* p_l)}{U_k U_k^* + \mathrm{Re}(a_{ijkl}U_i^* U_k p_l p_j^*)} \; . \tag{24}$$

Using equations (21)–(24) and the constraint relation (14), we can obtain certain useful relations. Multiplying (14) by U_i^*, we obtain

$$a_{ijkl}p_j p_l U_k U_i^* = U_i U_i^* \; . \tag{25}$$

Using (21) and (25), we then obtain

$$\mathbf{p}\cdot\mathbf{F} = 2K \; , \qquad \mathbf{p}^*\cdot\mathbf{F} = 2U - \mathrm{i}D_{diss} \; . \tag{26}$$

Equations (26) yield the projections of the Poynting vector $\mathbf{F}$ into the propagation vector $\mathbf{P}$ and into the attenuation vector $\mathbf{A}$, respectively:

$$\mathbf{P}\cdot\mathbf{F} = E - \tfrac{1}{2}\mathrm{i}D_{diss} \; , \qquad \mathbf{A}\cdot\mathbf{F} = \tfrac{1}{2}D_{diss} - \mathrm{i}(K - U) \; . \tag{27}$$

In terms of $\mathrm{Re}\mathbf{F}(=\mathbf{S})$ and $\mathrm{Im}\mathbf{F}$, Equations (27) may be expressed as follows:

$$\begin{aligned} &\mathbf{P}\cdot\mathbf{S} = E \; , && \mathbf{A}\cdot\mathbf{S} = \tfrac{1}{2}D_{diss} \; , \\ &\mathbf{P}\cdot\mathrm{Im}\mathbf{F} = -\tfrac{1}{2}D_{diss} \; , && \mathbf{A}\cdot\mathrm{Im}\mathbf{F} = U - K \; . \end{aligned} \tag{28}$$

All the equations given above are valid very generally, for homogeneous, inhomogeneous and bulk plane waves, for isotropic and anisotropic, elastic and viscoelastic media. They offer many important consequences. We list here several of them.

1) **The complete time-averaged energy** E. The complete time-averaged energy $E = K + U$ can be simply computed using (23). It can be, however, alternatively expressed in terms of $\mathbf{P}$ and $\mathbf{S}$, see (28),

$$E = K + U = \mathbf{P}\cdot\mathbf{S} = \tfrac{1}{2}\rho\omega^2 \mathrm{Re}(p_j)\mathrm{Re}(a_{ijkl}U_k U_i^* p_l) \exp[-2\omega A_n x_n] \; . \tag{29}$$

Thus, E is represented by the projection of the propagation vector $\mathbf{P}$ into the time-averaged energy flux vector $\mathbf{S}$. For $\mathbf{P}$ perpendicular to $\mathbf{S}$, E vanishes.

2) **Time-averaged dissipated energy** $D_{diss} = 2\mathbf{A}\cdot\mathbf{S} = -2\mathbf{P}\cdot\mathrm{Im}\mathbf{F}$. It is represented by the projection of the attenuation vector $\mathbf{A}$ into the time-averaged energy flux vector $\mathbf{S}$. Alternatively, $-D_{diss}$ is represented by a projection of the propagation vector $\mathbf{P}$ into the imaginary part of the Poynting vector, Im$\mathbf{F}$.

3) **Energy angle** i_{en}. It is introduced here as the angle between the propagation vector $\mathbf{P}$ (normal to the wavefront) and the time-averaged energy flux density $\mathbf{S}$,

$$\cos i_{en} = \mathbf{P}\cdot\mathbf{S}/|\mathbf{P}||\mathbf{S}| = E/|\mathbf{P}||\mathbf{S}| \geq 0 \ , \tag{30}$$

see (28). Consequently, the angle i_{en} is always less or equal to 90^0. Moreover, the complete time-averaged energy E is proportional to $\cos i_{en}$.

4) **Attenuation-energy angle** γ_{en}. It is introduced here as the angle between the attenuation vector $\mathbf{A}$ and the time-averaged energy flux $\mathbf{S}$,

$$\cos \gamma_{en} = \mathbf{A}\cdot\mathbf{S}/|\mathbf{A}||\mathbf{S}| = \tfrac{1}{2}D_{diss}/|\mathbf{A}||\mathbf{S}| \geq 0 \ , \tag{31}$$

see (28). Consequently, the angle γ_{en} does not exceed 90^0. Moreover, the time-averaged dissipated energy D_{diss} is proportional to $\cos \gamma_{en}$.

5) **The time-averaged energy velocity** $\boldsymbol{\mathcal{U}}$. It is given by (24), but can be also expressed in a simpler form using (29):

$$\mathcal{U}_i = \frac{S_i}{E} = \frac{S_i}{\mathbf{P}\cdot\mathbf{S}} = \frac{\mathrm{Re}(a_{ijkl}U_kU_j^*p_l)}{\mathrm{Re}(a_{ijkl}U_kU_i^*p_l)\mathrm{Re}(p_j)} \ . \tag{32}$$

6) **Expression for** $P_i\mathcal{U}_i$. It immediately follows from (32) that

$$\mathbf{P}\cdot\boldsymbol{\mathcal{U}} = 1 \ . \tag{33}$$

This equation represents a generalization of the important relation $\mathbf{p}\cdot\boldsymbol{\mathcal{U}} = 1$, where $\boldsymbol{\mathcal{U}}$ is the group velocity vector, known for plane waves propagating in perfectly elastic anisotropic media.

7) **Quality factor** Q. **Loss factor** $\mathcal{L}$. In isotropic viscoelastic media, the quality factor has been mostly introduced by the relation $Q = -\mathrm{Re}(M)/\mathrm{Im}(M)$, where M is the relevant complex-valued viscoelastic modulus. In anisotropic viscoelastic media, however, such a definition fails, see Krebes and Le (1994). It is more suitable to define the quality factor Q in terms of time-averaged energy quantities. Such a definition was introduced even for isotropic viscoelastic media by Buchen (1971). For example, the definition valid both for isotropic and anisotropic media, given by Carcione (2001, p.138), is as follows

$$Q = 2U/D_{diss} \ . \tag{34}$$

Using (28), we can express it in an alternative way,

$$Q = \frac{U}{A_iS_i} = \tfrac{1}{2}\,\frac{U_iU_i^*}{\mathrm{Re}(a_{ijkl}U_kU_j^*p_l)\mathrm{Im}(p_i)} \ . \tag{35}$$

We further introduce the loss factor $\mathcal{L}$ as the inverse of Q,

$$\mathcal{L} = Q^{-1} = 2\mathrm{Re}(a_{ijkl}U_k U_j^* p_l)\mathrm{Im}(p_i)/(U_i U_i^*) \ . \tag{36}$$

8) **Perfectly elastic anisotropic medium.** In perfectly elastic anisotropic medium (a_{ijkl} real-valued), the quantity $a_{ijkl}p_j p_l^* U_i U_k^*$, appearing in expressions for U and D_{diss}, see (23), is real-valued, for arbitrary complex-valued $\mathbf{p}$ and $\mathbf{U}$. This indicates that the time-averaged dissipated energy vanishes, $D_{diss} = 0$, see (23). From (28), we then obtain

$$\mathbf{A} \cdot \mathbf{S} = 0 \ , \qquad \mathbf{P} \cdot \mathrm{Im}\mathbf{F} = 0 \ . \tag{37}$$

In perfectly elastic isotropic media, the time-averaged energy flux $\mathbf{S}$ is always parallel to the propagation vector $\mathbf{P}$. It follows from (37) that both vectors $\mathbf{P}$ and $\mathbf{S}$ are perpendicular to the attenuation vector $\mathbf{A}$ and to the imaginary part of the Poynting vector Im$\mathbf{F}$.

4 Significant directions in plane wave propagation

In the propagation of scalar plane waves in non-dissipative media, there is only one significant direction of propagation, corresponding to the direction of (real-valued) slowness vector $\mathbf{p}$. For vectorial plane waves, the number of distinct directions is greater. It increases with the increasing complexity of the model (isotropic, anisotropic, perfectly elastic, viscoelastic).

Let us now briefly summarize the significant directions of vectorial plane waves propagating in viscoelastic anisotropic media:

a) The slowness vector $\mathbf{p}$. It is complex-valued, $\mathbf{p} = \mathbf{P} + \mathrm{i}\mathbf{A}$, with $\mathbf{P}$ and $\mathbf{A}$ oriented in generally different directions: the propagation vector $\mathbf{P}$ in the direction of propagation (perpendicular to the wavefront), and the attenuation vector $\mathbf{A}$ in the direction perpendicular to the plane of constant amplitudes.

b) The amplitude vector $\mathbf{U}$. In viscoelastic media, the relevant amplitude vector is complex-valued, $\mathbf{U} = \mathrm{Re}\mathbf{U} + \mathrm{i}\,\mathrm{Im}\mathbf{U}$. Consequently, the amplitude vector is specified by two real-valued, generally different directions, along Re$\mathbf{U}$ and Im$\mathbf{U}$.

c) The Poynting vector $\mathbf{F}$. It is complex-valued, so that it is specified by two real-valued, generally different directions, along Re$\mathbf{F}$ and Im$\mathbf{F}$. The vector Re$\mathbf{F}$ represents the time-averaged energy flux $\mathbf{S}$, and it points in the direction of the time-averaged energy velocity vector $\boldsymbol{\mathcal{U}}$, see (24). Both $\mathbf{S}$ and $\boldsymbol{\mathcal{U}}$ are real-valued.

If the above listed vectors are complex-valued, they may be either *homogeneous or inhomogeneous*. Let us now briefly specify the concept of homogeneous and inhomogeneous vectors.

Consider an arbitrary complex-valued vector $\mathbf{B} = \mathbf{C} + \mathrm{i}\mathbf{D}$, where $\mathbf{C}$ and $\mathbf{D}$ are real-valued vectors. We use the following terminology: $\mathbf{B}$ is called **homogeneous** complex-valued vector if the real-valued vectors $\mathbf{C}$ and $\mathbf{D}$ are parallel, and is called **inhomogeneous** if $\mathbf{C}$ and $\mathbf{D}$ are non-parallel. An example where this terminology has been often applied is the slowness vector $\mathbf{p} = \mathbf{P} + \mathrm{i}\mathbf{A}$. We call the slowness vector $\mathbf{p}$ a homogeneous

slowness vector if $\mathbf{P}$ and $\mathbf{A}$ are parallel, and inhomogeneous slowness vector if $\mathbf{P}$ and $\mathbf{A}$ are non-parallel. This terminology has been also extended for plane waves. If the slowness vector is homogeneous, the plane wave is called homogeneous, and if it is inhomogeneous, the plane wave is called inhomogeneous. The actual inhomogeneity of the plane wave is controlled by the inhomogeneity strength $|D|$. The plane wave is homogeneous for $|D| = 0$, weakly inhomogeneous for small $|D|$, and strongly inhomogeneous for $|D|$ large.

The term homogeneous and inhomogeneous can be used even for other complex-valued vectors. For example, the amplitude vectors of P, S1, and S2 waves are in general inhomogeneous, but the amplitude vector of an SH plane wave propagating in a plane of symmetry Σ^S is homogeneous, as its real and imaginary parts are parallel (perpendicular to the plane of symmetry Σ^S). Similarly, the Poynting vector $\mathbf{F}$ of plane waves is, in general, inhomogeneous. It may be, however, homogeneous for certain nonzero small values of D.

We will now briefly discuss a formally constructed complex-valued vector $\mathbf{s} = \mathbf{S} + \mathrm{i}g\mathbf{A}$. A real-valued positive constant g is introduced to obtain the same dimension of $g\mathbf{A}$ and $\mathbf{S}$. We call the complex-valued vector $\mathbf{s}$ the energy-attenuation vector. Its real part is the time-averaged energy flux, and imaginary part has the direction of the attenuation vector.

The energy-attenuation vector $\mathbf{s} = \mathbf{S} + \mathrm{i}g\mathbf{A}$ has certain interesting properties, which differ from the slowness vector $\mathbf{p} = \mathbf{P} + \mathrm{i}\mathbf{A}$. The differences are mainly between the attenuation angle γ (which measures the angle between $\mathbf{P}$ and $\mathbf{A}$) and the energy-attenuation angle γ_{en} (which measures the angle between $\mathbf{S}$ and $g\mathbf{A}$):

$$\cos\gamma = \mathbf{P}\cdot\mathbf{A}/|\mathbf{P}||\mathbf{A}| \ , \qquad \cos\gamma_{en} = \mathbf{S}\cdot\mathbf{A}/|\mathbf{S}||\mathbf{A}| \ . \tag{38}$$

It is well known that the attenuation angle γ behaves simply in isotropic viscoelastic media, where it is always less then 90^0. In anisotropic viscoelastic media, however, its behaviour is more complicated. The maximum attenuation angle γ^* is not necessarily 90^0, but may be less, equal or greater then 90^0. See a detailed investigation of γ in Červený and Pšenčík (2005a,b). Contrary to it, the behaviour of the energy-attenuation angle γ_{en} is simple; it is always less or equal 90^0, for unrestricted anisotropy and viscoelasticity, see (31). It does not depend on g.

5 Energy flux of SH plane waves

Equation (21) for the Poynting vector of plane waves can be used for unrestricted anisotropy and viscoelasticity, and for an unrestricted value of inhomogeneity parameter D. It generally requires to solve an algebraic equation of the sixth degree (17). Here we consider only a special case, corresponding to SH plane waves propagating in a plane of symmetry of a monoclinic (orthorhombic, hexagonal) viscoelastic anisotropic medium. In this case, the algebraic equation of the sixth degree (17) factorizes and yields a quadratic equation, which may be simply solved analytically. Consequently, certain properties of energy flux of SH waves can be simply studied analytically, and discussed in detail.

5.1 Slowness vector of SH plane waves

We consider a plane of symmetry Σ^S in a monoclinic anisotropic viscoelastic medium, and choose the Cartesian coordinate system x_i in such a way that the plane of symmetry Σ^S corresponds to the coordinate plane x_1x_3. We further assume that the propagation-attenuation plane $\Sigma^{\|}$ coincides with Σ^S, i.e. $p_2 = 0$. The propagation of SH plane waves is then controlled by three Voigt density-normalized viscoelastic moduli A_{44}, A_{66} and A_{46}. We introduce the 2×2 complex-valued matrix

$$\mathbf{A} = \begin{pmatrix} A_{66} & A_{46} \\ A_{46} & A_{44} \end{pmatrix} , \tag{39}$$

and assume that $\mathrm{Re}(\mathbf{A})$ is positive definite, and $\mathrm{Im}(\mathbf{A})$ negative definite or zero.

The constraint relation (15) for the slowness vector $\mathbf{p}$ for SH waves yields:

$$A_{66}p_1^2 + A_{44}p_3^2 + 2A_{46}p_1p_3 = 1 , \tag{40}$$

and the constraint relation (14) for the amplitude vector $\mathbf{U}$ yields

$$\mathbf{U}(p_n) = (0, U_2(p_n), 0)^T . \tag{41}$$

As expected, the amplitude vector $\mathbf{U}$ of SH plane waves is perpendicular to the symmetry plane Σ^S, and is homogeneous. The component U_2 may be complex valued. We also introduce the unit real-valued vectors $\mathbf{n}$ and $\mathbf{m}$ as follows:

$$\mathbf{n} = (n_1, 0, n_3)^T , \qquad \mathbf{m} = (n_3, 0, -n_1)^T . \tag{42}$$

As we can see, $\mathbf{n}$ and $\mathbf{m}$, given by (42), are mutually perpendicular.

The expressions for the slowness vector components p_1 and p_3 can be obtained by inserting (42) into (16):

$$p_1 = \sigma n_1 + \mathrm{i}Dn_3 , \qquad p_3 = \sigma n_3 - \mathrm{i}Dn_1 . \tag{43}$$

The quadratic equation (40) for σ then reads:

$$A_{66}(\sigma n_1 + \mathrm{i}Dn_3)^2 + A_{44}(\sigma n_3 - \mathrm{i}Dn_1)^2 + 2A_{46}(\sigma n_1 + \mathrm{i}Dn_3)(\sigma n_3 - \mathrm{i}Dn_1) = 1 . \tag{44}$$

It has two roots, σ_1 and σ_2,

$$\sigma_{1,2} = -\mathrm{i}D\Lambda/\Gamma_{22} \pm [1/\Gamma_{22} + D^2\Delta/\Gamma_{22}^2]^{1/2} , \tag{45}$$

where

$$\begin{aligned} \Gamma_{22} &= A_{66}n_1^2 + A_{44}n_3^2 + 2A_{46}n_1n_3 , \\ \Lambda &= (A_{66} - A_{44})n_1n_3 + A_{46}(n_3^2 - n_1^2) , \\ \Delta &= A_{44}A_{66} - A_{46}^2 . \end{aligned} \tag{46}$$

Once a quantity σ has been found, we can determine $\mathbf{P}, \mathbf{A}, |\mathbf{P}|, |\mathbf{A}|, \mathbf{N}, \mathbf{M}, \mathcal{C}$ and γ using the relation, see (19) and (20),

$$\begin{array}{ll} P_1 = n_1 \mathrm{Re}\sigma \ , & A_1 = n_1 \mathrm{Im}\sigma + n_3 D \ , \\ P_3 = n_3 \mathrm{Re}\sigma \ , & A_3 = n_3 \mathrm{Im}\sigma - n_1 D \ , \\ |\mathbf{P}| = |\mathrm{Re}\sigma| \ , & |\mathbf{A}| = [(\mathrm{Im}\sigma)^2 + D^2]^{1/2} \\ N_1 = \epsilon n_1 \ , & M_1 = [n_1 \mathrm{Im}\sigma + n_3 D]/[(\mathrm{Im}\sigma)^2 + D^2]^{1/2} \ , \\ N_3 = \epsilon n_3 \ , & M_3 = [n_3 \mathrm{Im}\sigma - n_1 D]/[(\mathrm{Im}\sigma)^2 + D^2]^{1/2} \ , \\ \mathcal{C} = 1/|\mathrm{Re}\sigma| \ , & \cos\gamma = \epsilon\, \mathrm{Im}\sigma/[(\mathrm{Im}\sigma)^2 + D^2]^{1/2} \ . \end{array} \tag{47}$$

We also get $P_2 = 0$, $A_2 = 0$, $N_2 = 0$, $M_2 = 0$.

5.2 Energy quantities of SH plane waves

Let us now discuss the Poynting vector $\mathbf{F}$ of SH plane waves. Using (21), we obtain

$$F_i = \tfrac{1}{2}\rho\omega^2 U_2 U_2^* a_{i2k2} p_k \exp[-2\omega A_n x_n] \ . \tag{48}$$

In the following, we shall consider the Poynting vector $\mathbf{F}$ in the normalized form:

$$F_i = A^F G_i \ , \tag{49}$$

where A^F is the normalization factor, given by the relation,

$$A^F = \tfrac{1}{2}\rho\omega^2 U_2 U_2^* \exp[-2\omega A_n x_n] \ . \tag{50}$$

The normalization factor A^F is always real-valued and positive, $A^F > 0$. Consequently, the normalized Poynting vector $\mathbf{G}$ of SH waves is given by a simple expression

$$G_i = a_{i2k2} p_k \ . \tag{51}$$

If we use the Voigt notation for the density-normalized complex-valued viscoelastic moduli, G_1 and G_3 are given by relations

$$G_1 = A_{66} p_1 + A_{46} p_3 \ , \quad G_3 = A_{46} p_1 + A_{44} p_3 \ . \tag{52}$$

Equations (52) represent the final expression for the normalized complex-valued Poynting vector of SH waves. We emphasize again that A_{44}, A_{66} and A_{46} are complex-valued, and that p_1, p_3 are also complex-valued and given by (18) with (47).

Using (50) and (52), we can express also other energy quantities of SH plane waves in terms of A^F and $\mathbf{G}$:

The time-averaged kinetic energy K, time-averaged strain energy U, and the time-averaged dissipated energy D_{diss} read:

$$K = \tfrac{1}{2}A^F \ , \quad U = \tfrac{1}{2}A^F \mathrm{Re}(\mathbf{G}\cdot\mathbf{p}^*) \ , \quad D_{diss} = -A^F \mathrm{Im}(\mathbf{G}\cdot\mathbf{p}^*) \ . \tag{53}$$

The time-averaged energy flux density $\mathbf{S}$, and the time-averaged energy velocity $\boldsymbol{\mathcal{U}}$,

$$\mathbf{S} = A^F \mathrm{Re}(\mathbf{G}) \ , \quad \boldsymbol{\mathcal{U}} = 2\mathrm{Re}(\mathbf{G})/[1 + \mathrm{Re}(\mathbf{G}\cdot\mathbf{p}^*)] \ . \tag{54}$$

The quality factor Q and the loss factor $\mathcal{L}$:

$$Q = 1/(2\mathbf{A}\cdot\mathrm{Re}\mathbf{G}) \ , \quad \mathcal{L} = 2\mathbf{A}\cdot\mathrm{Re}\mathbf{G} \ . \tag{55}$$

5.3 Significant directions in SH plane wave propagation

In this section, we shall pay attention mainly to energy-attenuation angle γ_{en} and to the Poynting vector of plane SH waves.

For SH waves, $\sin\gamma_{en}$ can be computed analytically:

$$\sin\gamma_{en} = |A_3 \mathrm{Re}G_1 - A_1 \mathrm{Re}G_3|/|\mathbf{A}||\mathrm{Re}\mathbf{G}| \ . \tag{56}$$

This yields, see (47) and (52),

$$\sin\gamma_{en} = |\mathrm{Re}\sigma[\mathrm{Im}\sigma\mathrm{Re}\Lambda - D\mathrm{Re}|\Gamma_{22}]|/|\mathbf{A}||\mathrm{Re}\mathbf{G}| \ . \tag{57}$$

Consider now weakly inhomogeneous plane waves (small $|D|$), and use approximately

$$\mathrm{Im}\sigma \doteq e - fD \ , \tag{58}$$

where

$$e = \mathrm{Im}(1/\Gamma_{22})^{1/2} \ , \qquad f = \mathrm{Re}(\Lambda/\Gamma_{22}) \doteq \mathrm{Re}(\Lambda)/\mathrm{Re}(\Gamma_{22}) \ . \tag{59}$$

see Červený and Pšenčík (2005a, Eqs. (66) and (67)). Inserting (58) into (57) yields

$$\sin\gamma_{en} = |\mathrm{Re}\sigma[e\mathrm{Re}\Lambda - D(f\mathrm{Re}\Lambda + \mathrm{Re}\Gamma_{22})]|/|\mathbf{A}||\mathrm{Re}\mathbf{G}| \ . \tag{60}$$

The energy-attenuation vector $\mathbf{s} = \mathbf{S} + \mathrm{i}g\mathbf{A}$ is homogeneous for such D, for which (60) vanishes. We denote such D for which $\mathbf{s}$ is homogeneous by D_{en}, and obtain for it a simple approximate result:

$$D_{en} \doteq ef/(1+f^2) \ . \tag{61}$$

It was shown in Červený and Pšenčík (2005a, Section 3.3(a)), that the same D as D_{en} in (61) has a very interesting property: The attenuation $|\mathbf{A}|$, as a function of D; is minimum for such D. For this reason, it is denoted by D_{att} in Červený and Pšenčík (2005a, Equation (71)).

The conclusion is: For weakly inhomogeneous plane waves, the attenuation $|\mathbf{A}|$, as a function of D (for fixed direction of propagation), is approximately minimum for the inhomogeneity parameter $D = D_{en}(= D_{att})$, for which the energy-attenuation vector $\mathbf{s} = \mathbf{S} + \mathrm{i}g\mathbf{A}$ is homogeneous. The direction of $\mathbf{A}$ is generally different from the propagation direction specified by $\mathbf{P}$, which means that the corresponding plane wave is inhomogeneous.

For SH plane waves, we can also determine the Poynting vector analytically. Analogously, it is also possible to determine analytically the angle γ_F between $\mathbf{S}$ and $\mathrm{Im}\mathbf{F}$,

$$\sin\gamma_F = |\mathrm{Re}G_1\mathrm{Im}G_3 - \mathrm{Re}G_3\mathrm{Im}G_1|/|\mathrm{Re}\mathbf{G}||\mathrm{Im}\mathbf{G}| \ . \tag{62}$$

After simple, but lengthy computations we obtain that $\sin\gamma_F \doteq 0$ for $D = D^M$, where

$$D^M \doteq \pm b/2c \ , \tag{63}$$

and where

$$b = \mathrm{Im}(\Lambda/\Gamma_{22}) \ , \qquad c = \tfrac{1}{2}\mathrm{Re}(\Delta/\Gamma_{22}^{3/2}) \ . \tag{64}$$

It was shown by Červený and Pšenčík (2005a, Section 3.4.7) that D^M also represents the inhomogeneity parameter for which the phase velocity (as a function of D) is maximum.

The conclusion is: For weakly inhomogeneous plane waves, the phase velocity $\mathcal{C}$, as a function of D (for fixed direction of propagation), is approximately maximum for the inhomogeneity parameter $D = D^M$, for which the Poynting vector $\mathbf{F}$ is homogeneous.

6 Numerical examples for SH waves

In this section, we present several numerical examples related to the time-averaged energy flux S in viscoelastic anisotropic media. We consider the simplest possible case of inhomogeneous plane waves propagating in viscoelastic anisotropic media, namely the inhomogeneous SH plane waves propagating in a plane of symmetry of an anisotropic monoclinic (orthorhombic, hexagonal) viscoelastic medium, see Section 5.

In this case, the viscoelastic anisotropic medium is fully specified by three complex-valued, density-normalized Voigt moduli A_{44}, A_{66} and A_{46}. The properties of the complex-valued slowness vector $\mathbf{p}$ and of related real-valued quantities (propagation vector $\mathbf{P}$, attenuation vector $\mathbf{A}$, phase velocity $\mathcal{C}$, attenuation $|\mathbf{A}|$, the value of $\mathrm{Im}\sigma$, and the attenuation angle γ) of inhomogeneous SH plane waves propagating in such medium, are numerically investigated in Červený and Pšenčík (2005b, Section 3). We will supplement here these studies by studies of time-averaged energy flux vector $\mathbf{S}$ and by some related quantities (energy velocity $\mathcal{U}$, loss factor $\mathcal{L}$, energy direction i_{en}, and energy-attenuation angle γ_{en}).

Model 1 is defined by the following moduli:

$$A_{44} = 5 - \mathrm{i}\ , \quad A_{66} = 11.25 - 1.125\mathrm{i}\ , \quad A_{46} = 2.5\ . \tag{65}$$

All quantities in (65) are expressed in dimensions $(\mathrm{km/s})^2$. They fully correspond to those given in Equation (20) of Červený and Pšenčík (2005b). They are also very close to those used in Carcione and Cavallini (1995). The dissipation parameters (i.e., the imaginary parts of A_{44}, A_{66} and A_{46}) considered in (65) are rather strong. We therefore consider also three other models, with decreasing dissipation parameters (similarly as in Červený and Pšenčík, 2005b):
Model 2:

$$A_{44} = 5 - 0.5\mathrm{i}\ , \quad A_{66} = 11.25 - 0.5625\mathrm{i}\ , \quad A_{46} = 2.5\ , \tag{66}$$

Model 3:

$$A_{44} = 5 - 0.25\mathrm{i}\ , \quad A_{66} = 11.25 - 0.28125\mathrm{i}\ , \quad A_{46} = 2.5\ , \tag{67}$$

Model 4:

$$A_{44} = 5\ , \quad A_{66} = 11.25\ , \quad A_{46} = 2.5\ . \tag{68}$$

Model 4 represents a perfectly elastic anisotropic medium, with $\mathrm{Im}A_{44} = \mathrm{Im}A_{66} = \mathrm{Im}A_{46} = 0$.

Figures 1–6 display four plots each. From the top to the bottom, they show: a) the energy velocity $\mathcal{U}$, given by (32), b) the energy angle i_{en}, given by (30), representing the angle between the time-averaged energy flux $\mathbf{S}$ and the propagation vector $\mathbf{P}$, c) the loss factor $\mathcal{L}$, given by (36), d) the attenuation-energy angle γ_{en}, given by (31), and representing the angle between the attenuation vector $\mathbf{A}$ and the time-averaged energy flux $\mathbf{S}$.

The colour convention used in Figs. 1–5 corresponds exactly to that used in Červený and Pšenčík (2005b): the black curves correspond to Model 1, red curves to Model 2, green curves to Model 3, and blue curves to Model 4 (perfectly elastic). Thus, it is simple to compare the quantities related to the slowness vector $\mathbf{p}$ (Červený and Pšenčík, 2005b), and to the time-averaged energy flux $\mathbf{S}$.

The quantities under investigation are presented as function of: a) inhomogeneity parameter D, $-\infty < D < \infty$. b) Propagation angle i, $0 \leq i \leq 360^0$, related to the propagation vector $\mathbf{P}$, and given by equations

$$n_1 = \sin i \ , \quad n_2 = 0 \ , \quad n_3 = \cos i \ . \tag{69}$$

Consequently, the two types of figures are presented: a) For the propagation angle i fixed, and inhomogeneity parameter D varying, see Section 6.1. b) For the inhomogeneity parameter D fixed, but the propagation angle i varying (polar graphs), see Section 6.2. Let us emphasize that the propagation angle i is related to the direction of the propagation of the wavefront, not to the direction of the energy propagation.

6.1 Dependence on the inhomogeneity parameter D, the propagation angle i fixed

Similarly as in Červený and Pšenčík (2005b), we consider two propagation angles: $i = 45^0$ (in Figs. 1 and 2) and $i = 135^0$ (in Figs. 3 and 4).

In Fig. 1, the same input data are used as in Fig. 2 of Červený and Pšenčík (2005b), so that the computed quantities in both figures can be directly related. The inhomogeneity parameter D varies from -0.2 to 0.2. As we are mostly interested in weakly inhomogeneous plane waves (D small), the region $D \in (-0.2, 0.2)$ is quite sufficient for our studies: As the energy angle i_{en} and the attenuation-energy angle γ_{en} display certain interesting peculiarities for very small values of D, we also include Fig. 2, which shows details of the curves from Fig. 1 for very small values of D, varying from -0.03 to 0.03. Common feature of all these plots is that they are non-symmetric with respect to $D = 0$.

The **energy velocity** $\mathcal{U}$ varies quite smoothly as a function of D. It has a maximum at $D = 0$ (or very close to it), and decreases with the increasing inhomogeneity strength $|D|$. The distinct shift of the maximum of energy velocity from $D = 0$ to some non-zero D, observed for phase velocities $\mathcal{C}$, is observed also for energy velocity $\mathcal{U}$, but is only slight.

Let us now discuss the **energy angle** i_{en}. For weakly dissipative media, the energy angle is practically constant, independent of D. It is close the value of i_{en}, computed for perfectly elastic anisotropic medium. In our model, $i_{en} \doteq 16.4^0$ for perfectly elastic anisotropic medium. For viscoelastic media, i_{en} varies approximately linearly with D. With increasing dissipation, the slope of the straight line $i_{en}(D)$ increases.

The **loss factor** $\mathcal{L}$ depends strongly on dissipation. It is zero for perfectly elastic media. In viscoelastic media, for D given, it increases with increasing dissipation. For a given model, it is minimum for $D = 0$, and increases with increasing $|D|$. It can be taken as a measure of dissipation in the viscoelastic anisotropic medium.

The **energy-attenuation angle** γ_{en} has different properties than the attenuation angle γ. It is always less or equal 90^0, whereas the attenuation angle γ may be greater, equal or smaller than 90^0. This means that the amplitudes never increase in the direction of energy flux $\mathbf{S}$, as it might be the case in the direction of the propagation vector $\mathbf{P}$, see Červený and Pšenčík (2005b). For perfectly elastic anisotropic media, γ_{en} is independent

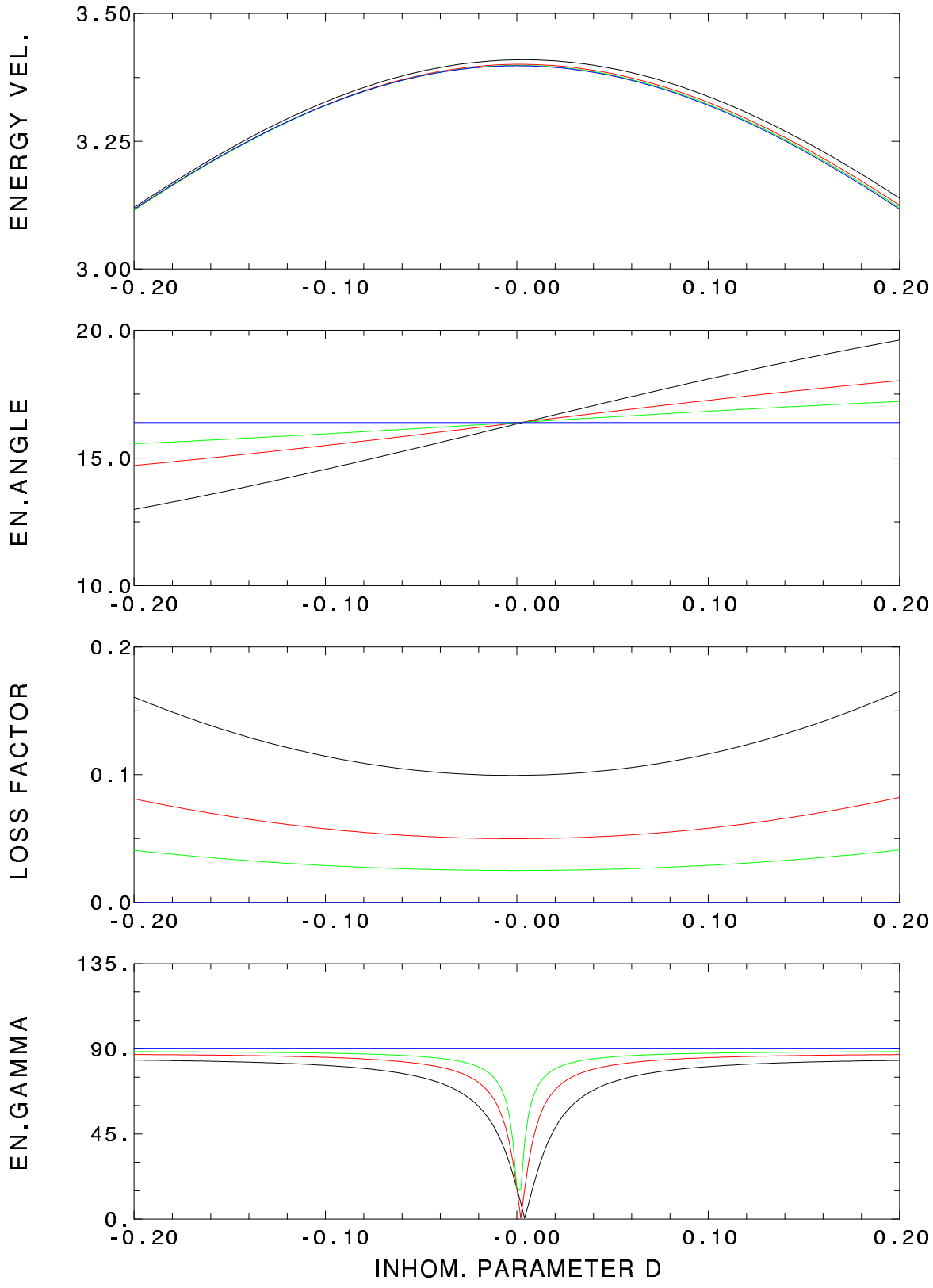
ENERGY VEL.
3.50
3.25
3.00
EN.ANGLE
20.0
15.0
10.0
LOSS FACTOR
0.2
0.1
0.0
EN.GAMMA
135.
90.
45.
0.
-0.20
-0.10
-0.00
0.10
0.20
INHOM. PARAMETER D
CA-DATA11

Figure 1

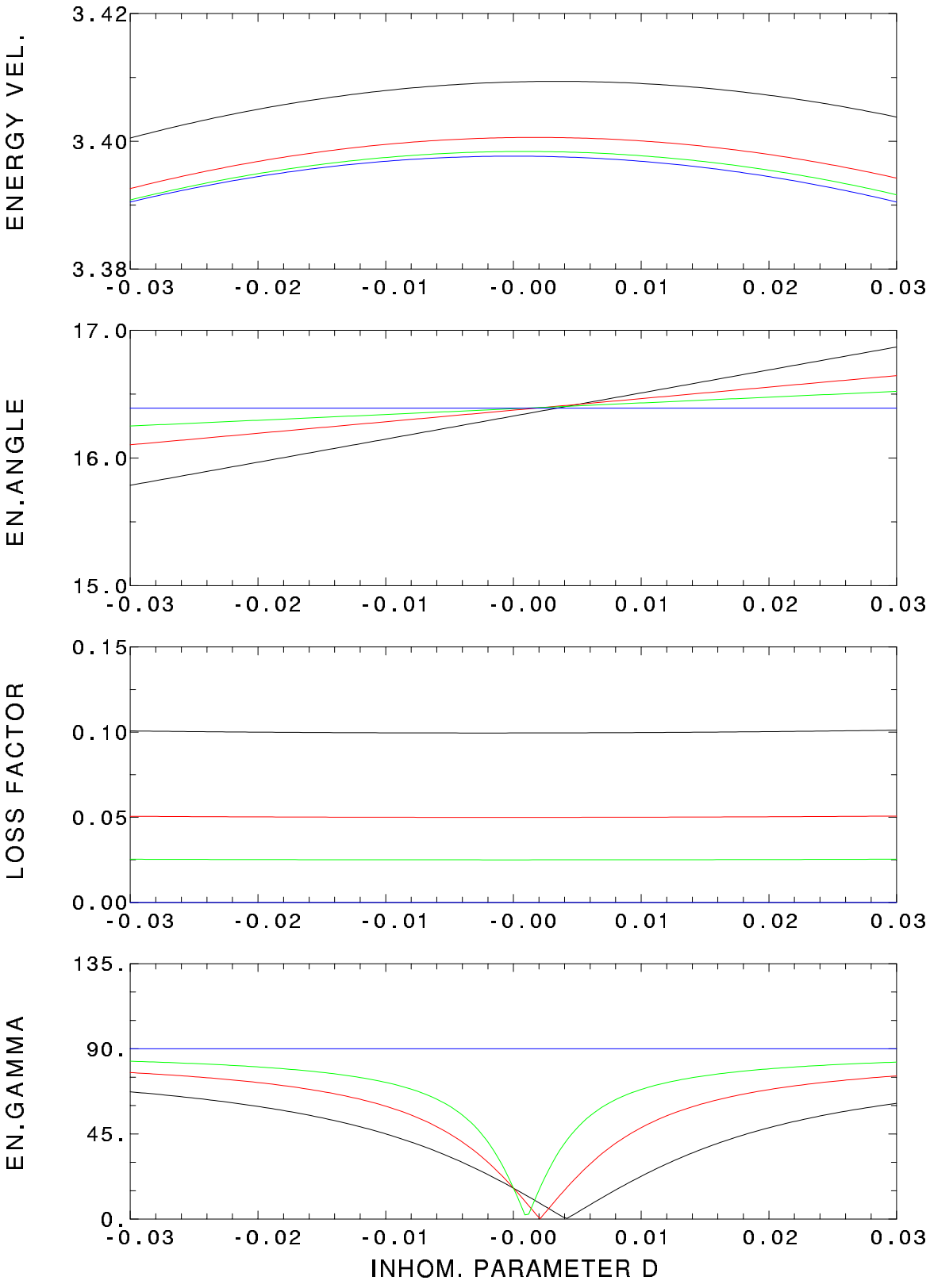
ENERGY VEL.
3.42
3.40
3.38
EN.ANGLE
17.0
16.0
15.0
LOSS FACTOR
0.15
0.10
0.05
0.00
EN.GAMMA
135.
90.
45.
0.
-0.03
-0.02
-0.01
-0.00
0.01
0.02
0.03
INHOM. PARAMETER D
CA-DATA21

Figure 2

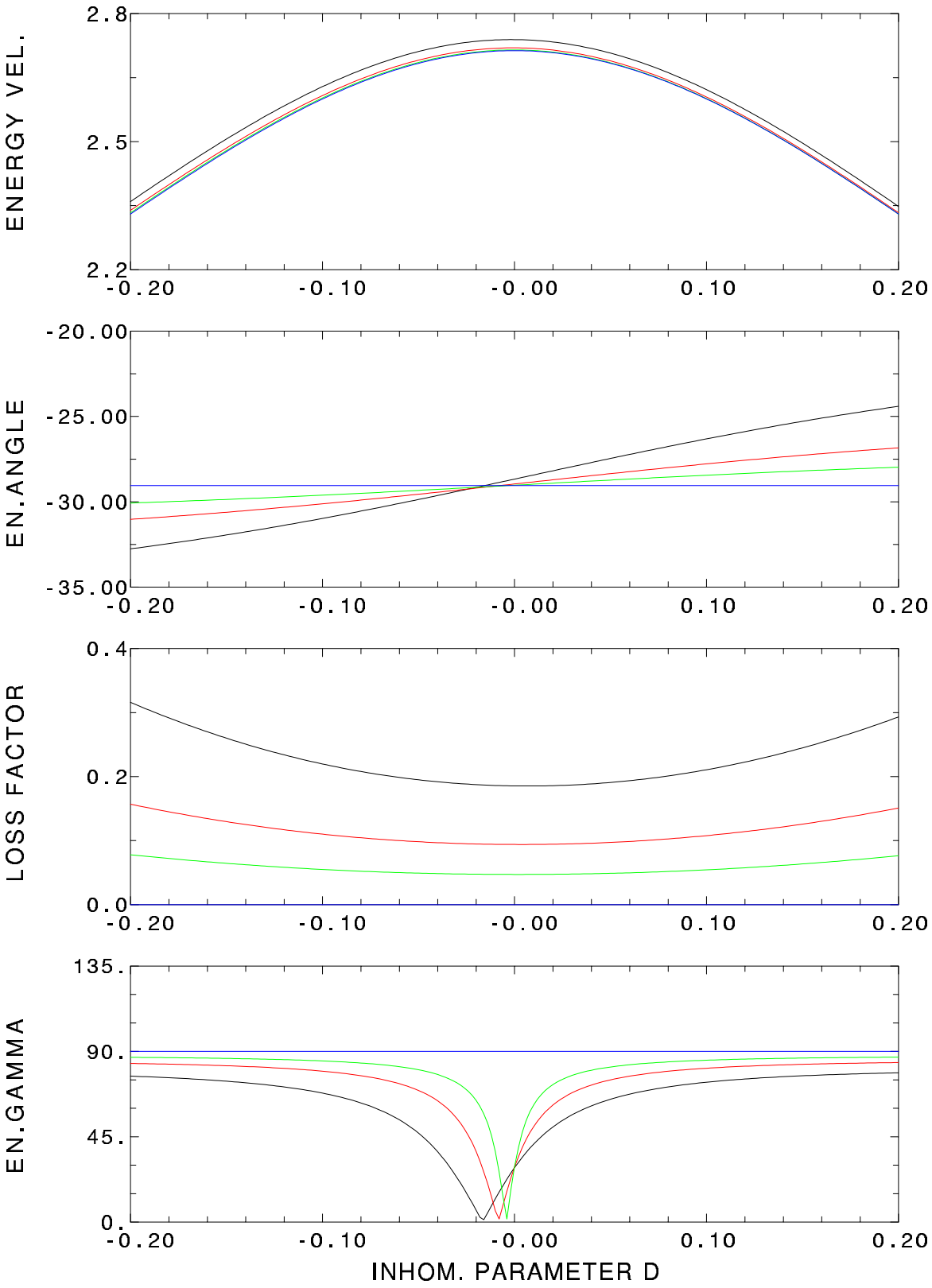
ENERGY VEL.
2.8
2.5
2.2
-0.20
-0.10
-0.00
0.10
0.20
EN.ANGLE
-20.00
-25.00
-30.00
-35.00
LOSS FACTOR
0.4
0.2
0.0
EN.GAMMA
135.
90.
45.
0.
INHOM. PARAMETER D
CA-DATA12

Figure 3

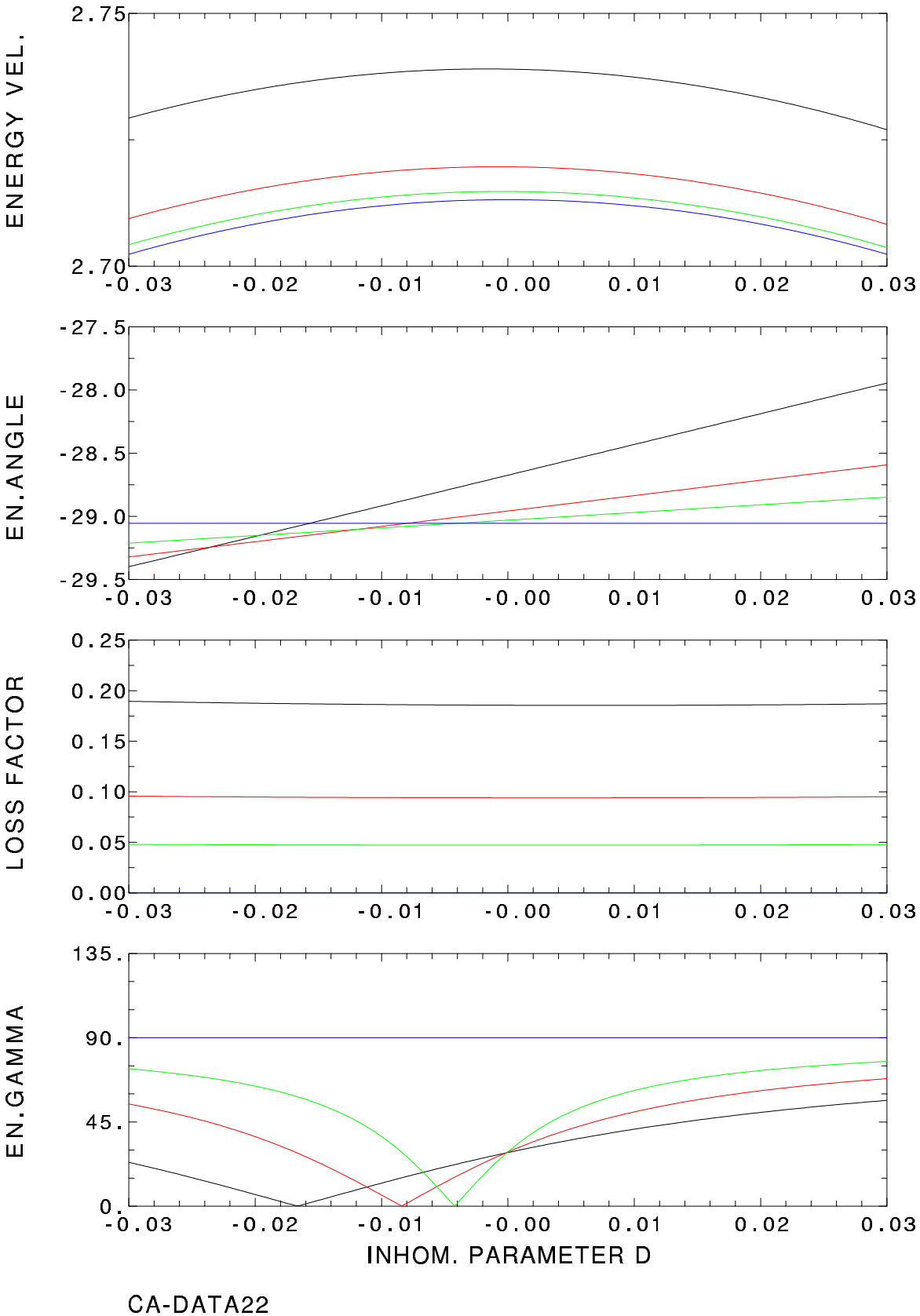
ENERGY VEL.
2.75
2.70
-0.03
-0.02
-0.01
-0.00
0.01
0.02
0.03
EN.ANGLE
-27.5
-28.0
-28.5
-29.0
-29.5
LOSS FACTOR
0.25
0.20
0.15
0.10
0.05
0.00
EN.GAMMA
135.
90.
45.
0.
INHOM. PARAMETER D
CA-DATA22

Figure 4

of D and equals 90^0. For fixed propagation angle i and D varying, there is always a (small) $D = D_{en}$, for which the energy-attenuation angle γ_{en} equals zero. It was shown in Section 5.3 that this D corresponds to that for which the attenuation $|\mathbf{A}|$ is minimum. The value of D_{en} can be approximated by (61) with (59).

Figs. 3 and 4 correspond to the propagation angle $i = 135^0$. All the conclusions obtained for $i = 45^0$ remain valid even for $i = 135^0$. Some effects are even more pronounced in Figs. 3, 4 than in Figs. 1, 2. For example, see the values of γ_{en} and relevant D_{en} in Fig. 4.

6.2 Dependence on the propagation angle i, inhomogeneity parameter D fixed

Here we discuss the propagation of homogeneous/inhomogeneous plane SH waves in a symmetry plane of a monoclinic anisotropic medium, as a function of the propagation angle i, for selected fixed values of inhomogeneity parameter D. We use the polar graphs, with $i = 0^0$ upwards, $i = 90^0$ to the right, etc., see (69). In pictures for the energy angle i_{en}, we present the absolute value of i_{en}. The three other quantities $(\mathcal{U}, \mathcal{L}, \cos\gamma_{en})$ are always non-negative.

In Fig. 5, the four curves in individual plots correspond to the four models (Model 1 - Model 4), and to fixed inhomogeneity parameter $D = 0.2$. The same colour convention is used as in Fig. 1 - Fig. 4: Blue corresponds to the perfectly elastic Model 4, black, red and green successively to Model 1, 2 and 3.

The plots of energy velocity $\mathcal{U}$ and energy angle i_{en} display a very small influence of dissipation on the result. The curves for all three models 1, 2, 3 show practically the same $\mathcal{U}$ and i_{en} as those for perfectly elastic media (Model 4). The polar graphs for energy velocity $\mathcal{U}$ are quite smooth, and have a bean-like shape. The form and size of the energy-velocity plots is very similar to the form and size of the phase-velocity plots, see Fig. 4 of Červený and Pšenčík (2005b). The polar graphs for the energy angle i_{en} have four lobes. The energy angle i_{en} changes sign approximately at directions corresponding to the axes of the bean-like polar graph of energy velocity $\mathcal{U}$.

The polar plot for the loss factor $\mathcal{L}$ is again of a bean-like shape, but is 90^0 rotated with respect to the polar plot of $\mathcal{U}$. Consequently, the loss factor is maximum for propagation angles i, for which the energy velocity $\mathcal{U}$ is minimum, and vice versa. The loss factor depends strongly on the anelasticity parameters. For perfectly elastic medium, the loss factor is zero, and for the increasing dissipation it increases. Thus, $\mathcal{L}$ can be taken as a measure of the dissipation, for given model and inhomogeneity parameter D.

The polar plots of $\cos(\gamma_{en})$ show again a smooth variation with the angle i. For a perfectly elastic medium (Model 4), $\gamma_{en} = 90^0$ for any i. For dissipative models, the values of $\cos(\gamma_{en})$ increase with increasing dissipation, being largest for, approximately, $i = 0^0$ and $i = 180^0$. For Model 1, $\gamma_{en} = 0$ in these directions.

Fig. 6 corresponds to the strongly dissipative Model 1, see Equation (65). The black curves correspond to $D = 0$ (perfectly elastic medium), the red curves to $D = 0.001$,

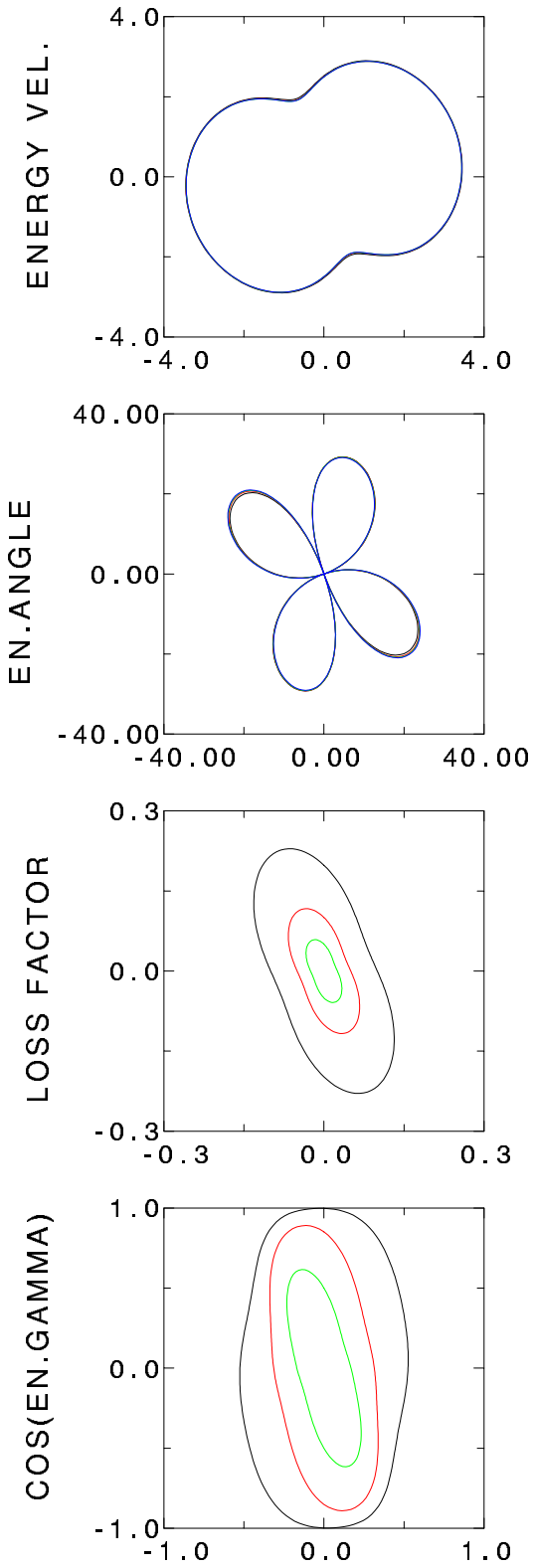
ENERGY VEL.
4.0
0.0
-4.0
-4.0
0.0
4.0
EN.ANGLE
40.00
0.00
-40.00
-40.00
0.00
40.00
LOSS FACTOR
0.3
0.0
-0.3
-0.3
0.0
0.3
COS(EN.GAMMA)
1.0
0.0
-1.0
-1.0
0.0
1.0
CA-DATA13

Figure 5

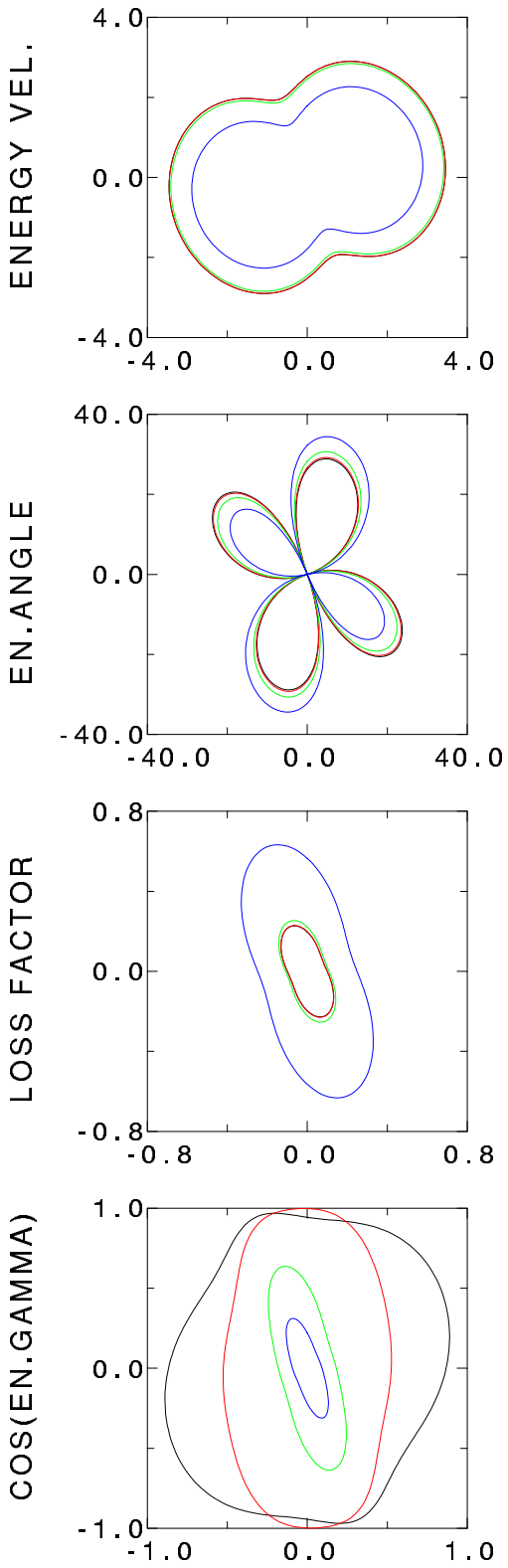
ENERGY VEL.
4.0
0.0
-4.0
-4.0
0.0
4.0
EN.ANGLE
40.0
0.0
-40.0
-40.0
0.0
40.0
LOSS FACTOR
0.8
0.0
-0.8
-0.8
0.0
0.8
COS(EN.GAMMA)
1.0
0.0
-1.0
-1.0
0.0
1.0
CA-DATA14

Figure 6

the green curves to $D = 0.005$, and the blue curves to $D = 0.01$. The most important observation is that the shape of individual curves in Fig. 6 remains very similar to that in Fig. 5. Consequently, the behaviour of $\mathcal{U}$, i_{en}, $\mathcal{L}$ and γ_{en} described in Section 6.1 has a more general character, at least for SH waves.

7 Plane waves in general viscoelastic anisotropic media

In the preceding sections we considered the case of SH waves propagating in a symmetry plane of a viscoelastic anisotropic medium, which allows derivation of explicit analytic formulae and their simple analysis. In this section we present and discuss results based on the determination of corresponding slowness vectors through the numerical solution of Eq.(17). In this way, we can investigate homogeneous and inhomogeneous plane waves propagating in arbitrary isotropic or anisotropic, perfectly elastic or anelastic media. We concentrate on inhomogeneous and homogeneous plane waves propagating in a cracked porous/permeable medium of hexagonal symmetry whose moduli were obtained by Jakobsen et al. (2003), or on its perfectly elastic counterpart, see below. A matrix material of quartz is containing two sets of communicating pores. The first set consists of spherical pores; the second set consists of (randomly oriented) flat pores. In addition, the model includes a relatively high concentration of flat cracks that are nearly fully aligned. For more details, see Jakobsen et al. (2003, p.231). We choose the model corresponding to the frequency of approximately 35 Hz shown in their Fig.2. For simplicity, we consider the density of 1000 kg/m^3. The matrix of complex-valued, density-normalized viscoelastic moduli of hexagonal symmetry with vertical axis of symmetry, measured in (km/s)^2 then reads:

$$\mathbf{A} = \mathbf{A_1} - \mathrm{i}\mathbf{A_2}, \tag{70}$$

where

$$\mathbf{A_1} = \begin{pmatrix} 46.631 & 5.983 & 4.278 & 0. & 0. & 0. \\ & 46.631 & 4.278 & 0. & 0. & 0. \\ & & 19.931 & 0. & 0. & 0. \\ & & & 13.444 & 0. & 0. \\ & & & & 13.444 & 0. \\ & & & & & 20.324 \end{pmatrix}$$

and

$$\mathbf{A_2} = \begin{pmatrix} 0.033 & 0.022 & 0.156 & 0. & 0. & 0. \\ & 0.033 & 0.156 & 0. & 0. & 0. \\ & & 1.312 & 0. & 0. & 0. \\ & & & 0.055 & 0. & 0. \\ & & & & 0.055 & 0. \\ & & & & & 0.005 \end{pmatrix}.$$

Note that both matrices $\mathbf{A_1}$ and $\mathbf{A_2}$ are positive definite. We calculate energy velocities $\mathcal{U}_i$, see (24), energy angle i_{en}, see (30), attenuation energy angle γ_{en}, see (31) and the loss factor $\mathcal{L}$, see (36) of a P wave and two S waves propagating in the plane of symmetry of the

medium specified by the above set of moduli. Note that we could extend this study out of the symmetry plane without any problem. We concentrate on it because behaviour of listed quantities can be better studied in it. For comparison, in addition to the quantities specifying plane wave propagation in the above viscoelastic anisotropic medium, we also calculate these quantities in a perfectly elastic anisotropic medium specified by the matrix $\mathbf{A_1}$ only. We first study the energy velocity as a function of propagation angle i with D fixed, then we study all the above listed parameters as functions of the inhomogeneity parameter D, with the propagation angle i fixed.

7.1 Dependence on the propagation angle i, inhomogeneity parameter D fixed

In Figs.7 and 8, we study energy velocities of the P and S waves as functions of the propagation angle i for several selected values of the inhomogeneity parameter D in the symmetry plane of the model of the viscoelastic anisotropic medium (70). The propagation-attenuation plane, it is plane formed by the vectors $\mathbf{n}$ and $\mathbf{m}$, coincides with the symmetry plane. The colours distinguish phases according to their phase velocities. The red colour indicates the fastest, the black colour intermediate and blue colour the slowest wave. It was shown in Červený and Pšenčík (2005b) that the red colour in the model (70) always corresponds to the P wave, the black colour corresponds mostly to the SH wave, only close to the vertical axis it may sometimes correspond to the SV wave. We present polar plots, in which $i = 0^0$ upwards, $i = 90^0$ to the right, see Eq.(69).

In Fig.7, **energy-velocity** polar graphs for six values of the inhomogeneity parameter D are shown: $D = 0$ (homogeneous wave), $D = 0.02$, $D = 0.06$, $D = 0.08$, $D = 0.1$ and $D = 0.2$. For $D = 0$, the energy-velocity surfaces are symmetric with respect to the vertical axis. The fastest (red) energy-velocity surface is separated from the remaining surfaces and corresponds to the P wave. The higher of the remaining S-wave velocities corresponds to the SH wave, the slower to the SV wave. Both S-wave energy velocities are equal along the vertical axis. Note that the plot resembles the phase-velocity plot for $D = 0$ in Fig.7 of Červený and Pšenčík (2005b). For increasing values of D, the P-wave and SV-wave energy velocity surfaces have some features similar with phase-velocity surfaces. With increasing D, the form of the surfaces becomes complicated in a vicinity of the vertical axis and the surfaces of P and S waves approach each other; with increasing D, the energy velocities decrease and plots become non-symmetric with respect to the vertical axis. There are, however, also some features, which distinguish the energy-velocity surfaces from the phase-velocity ones. We can see that with increasing D, the energy velocity of the P wave does not point into directions close to the vertical axis, see plots for $D = 0.06$ and greater. The energy-velocity surface of the P wave continuously changes into the energy-velocity surface of the faster of the two S waves. It is obvious that behaviour of weakly inhomogeneous waves in a vicinity of the vertical axis deserves more detailed study.

Fig.8 shows the same plots as Fig.7 but for plane waves propagating in a perfectly elastic anisotropic medium specified by the matrix $\mathbf{A_1}$ only, see (70). We can see that the basic character of all the plots in Fig.8 is similar to that in Fig.7. A significant difference between both figures is preserved symmetry of all the plots in Fig.8 (even for non-zero D)

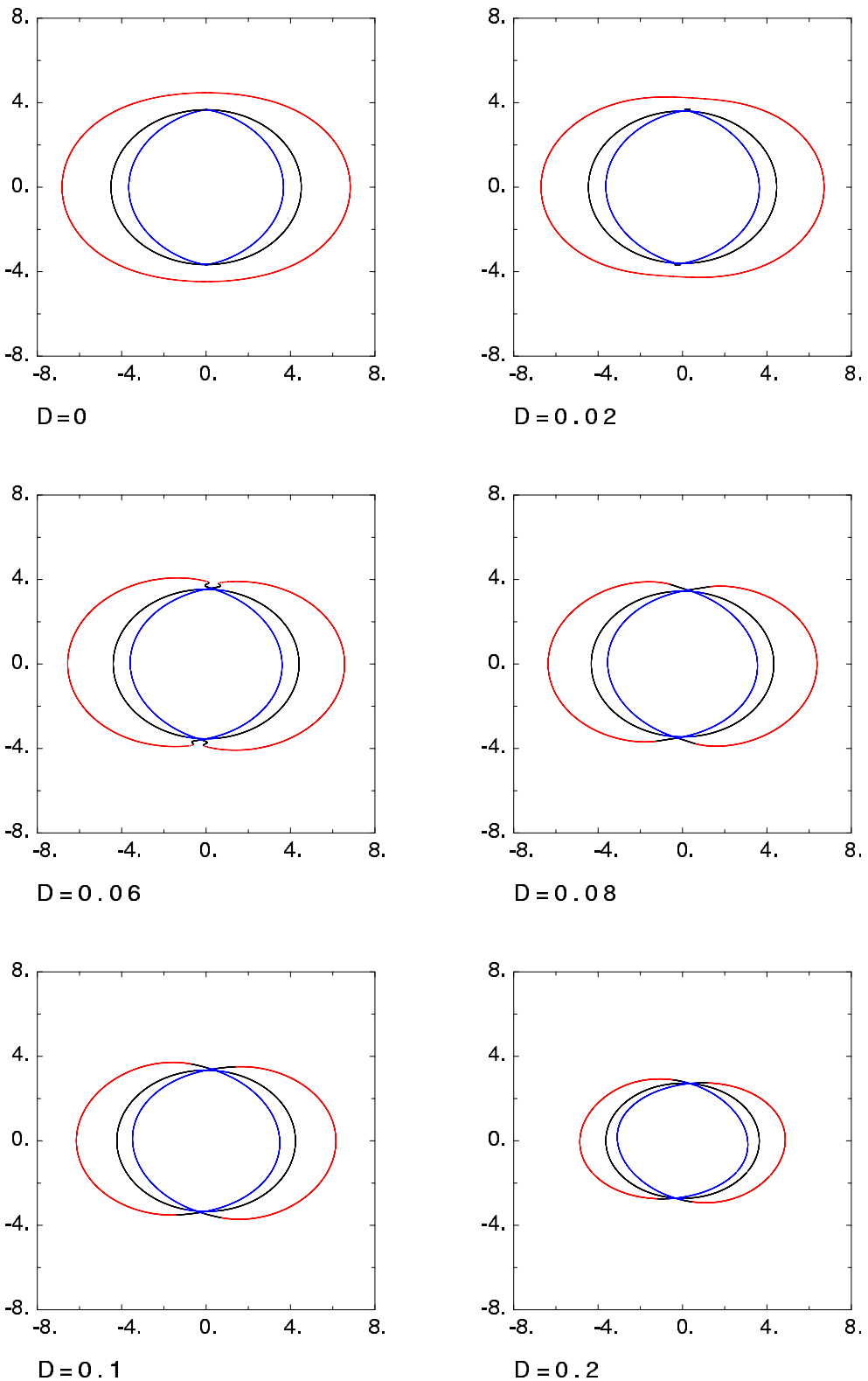

Figure 7

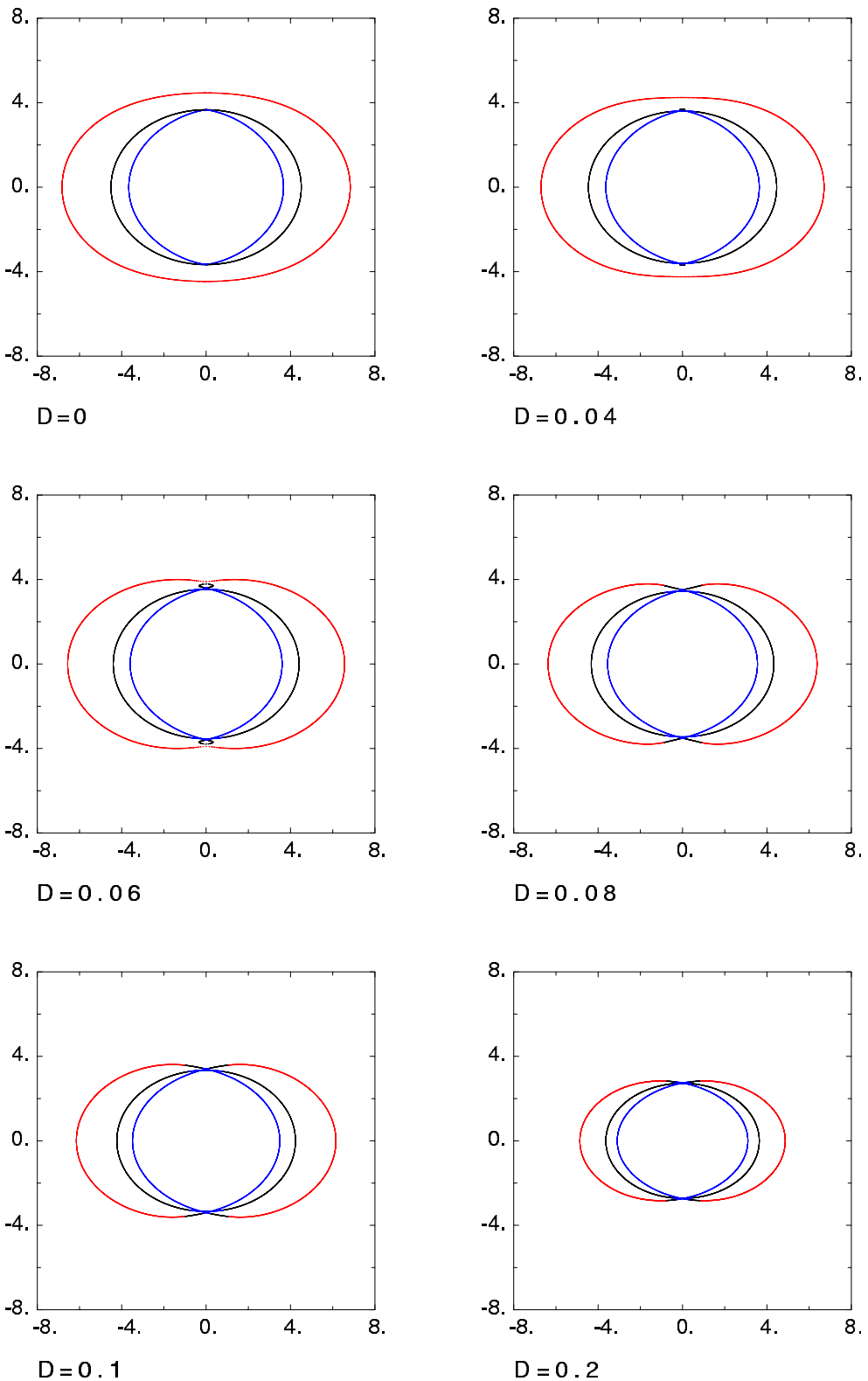

Figure 8

with respect to the vertical axis. Similarity of the plots in both figures seems to indicate that approximate approaches, in which imaginary parts of the viscoelastic moduli, i.e., elements of the matrix $\mathbf{A_2}$, are considered as perturbations, should work well.

In viscoelastic or perfectly elastic *isotropic* media, the sections of energy-velocity surfaces of both P and S waves would be circular.

7.2 Dependence on the inhomogeneity parameter D, the propagation angle i fixed

In Fig.9, we can see the variation of the **energy velocity**, in the plane of symmetry of the model of the viscoelastic anisotropic medium (70). The propagation-attenuation plane coincides again with the symmetry plane. Four values of the propagation angle are considered: $i = 0^0$, $i = 5^0$, $i = 10^0$ and $i = 45^0$, and the inhomogeneity parameter D varies from -0.2 to 0.2. The red colour corresponds again to the fastest wave, and according to Červený and Pšenčík (2005b), it is the P wave. The black colour corresponds to the faster of the S waves and the blue colour is reserved for the slowest wave. Fig.9 confirms what we saw in Fig.7. For propagation angles close to the vertical axis, behaviour of energy velocities as a function of D is more complicated than, for example, for the propagation angle $i = 45^0$. Only for the propagation angle $i = 45^0$, behaviour of the plots is similar to that of SH waves in Figs.1 and 3.

First feature which we can observe in Fig.9 is that the plots are non-symmetric with respect to $D = 0$ for the propagation angles $i = 5^0$, $i = 10^0$ and $i = 45^0$. It is most pronounced for the propagation angle $i = 5^0$. On the contrary for $i = 0^0$, the plot is fully symmetric.

Except for $i = 0^0$, we can observe a shift of the maximum of the energy velocity from $D = 0$ to a non-zero value of D. See similar observation for SH wave in Fig.1.

An interesting feature is decrease of the SV-wave energy velocity around $D = 0$ for $i = 0^0$ and partially also for $i = 5^0$. Another interesting feature is coincidence of shear-wave energy velocities for certain ranges of D.

For comparison, Fig.10 shows the same as Fig.9 but for plane waves propagating in a perfectly elastic medium. As in case of Figs.7 and 8, we can observe many similarities. The most distinguishable feature is strict symmetry of all plots in Fig.10 with respect to $D = 0$. Another interesting feature distinguishing Figs.9 and 10 is coincidence of energy velocities of P wave and SV wave for, approximately, $|D| > 0.06$ and their abrupt separation for smaller values of $|D|$ in the plot for $i = 0^0$.

Fig.11 shows behaviour of the **energy angle** as a function of D. We can see that only the plot for $i = 45^0$ resembles corresponding plots for the SH wave in Figs.1 and 3. For other directions of the propagation angle, behaviour of energy angles is more complicated. For $i = 0^0$ and for the slower S wave, which is an SH wave in this case, the energy angle is independent of D and zero, i.e., the directions of energy-velocity vector and the propagation vector are the same. For the P wave and the SV wave, the energy angle is zero for $D = 0$ and increases, with opposite signs for increasing $|D|$. For $|D| = 0.2$,it

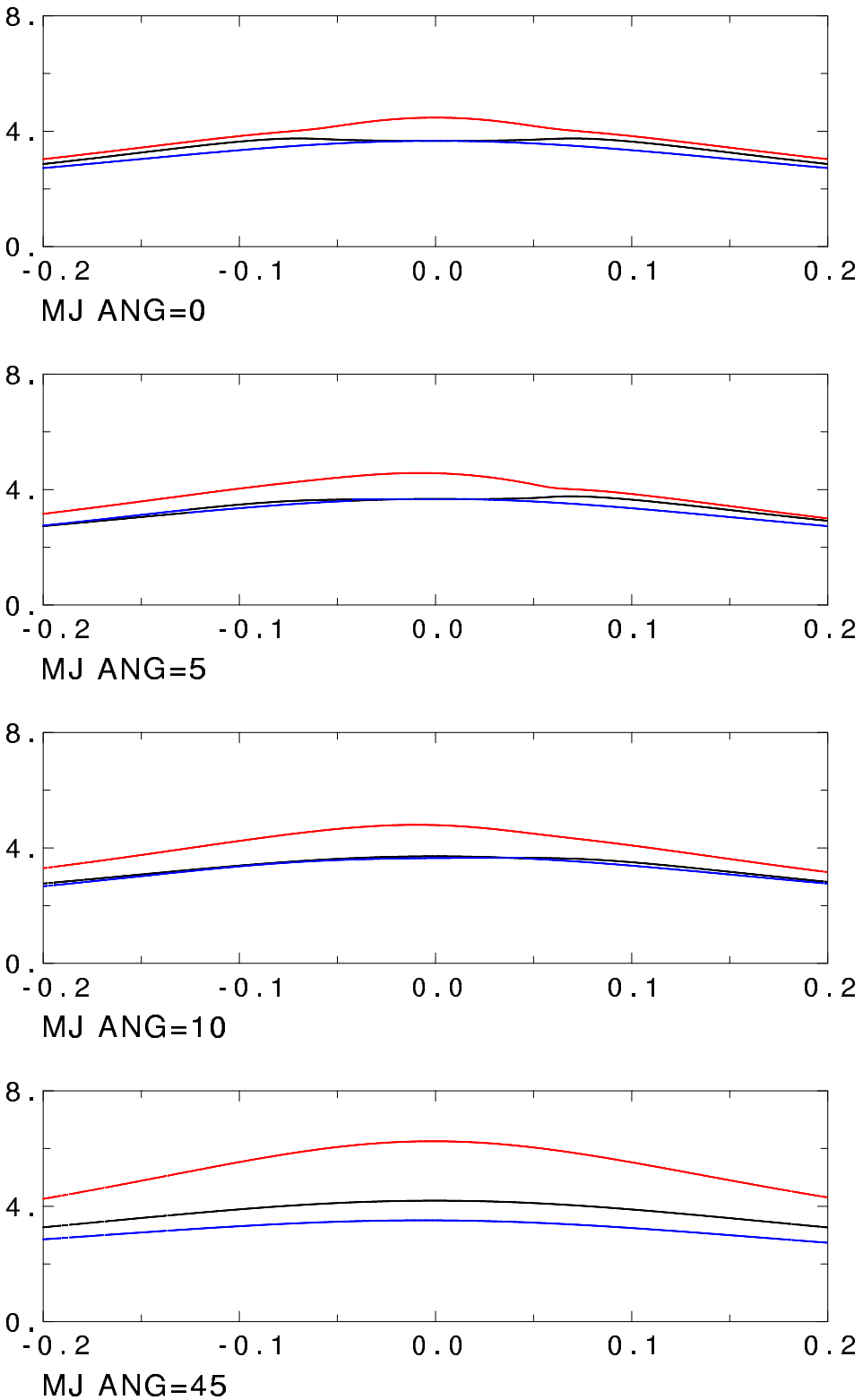

Figure 9

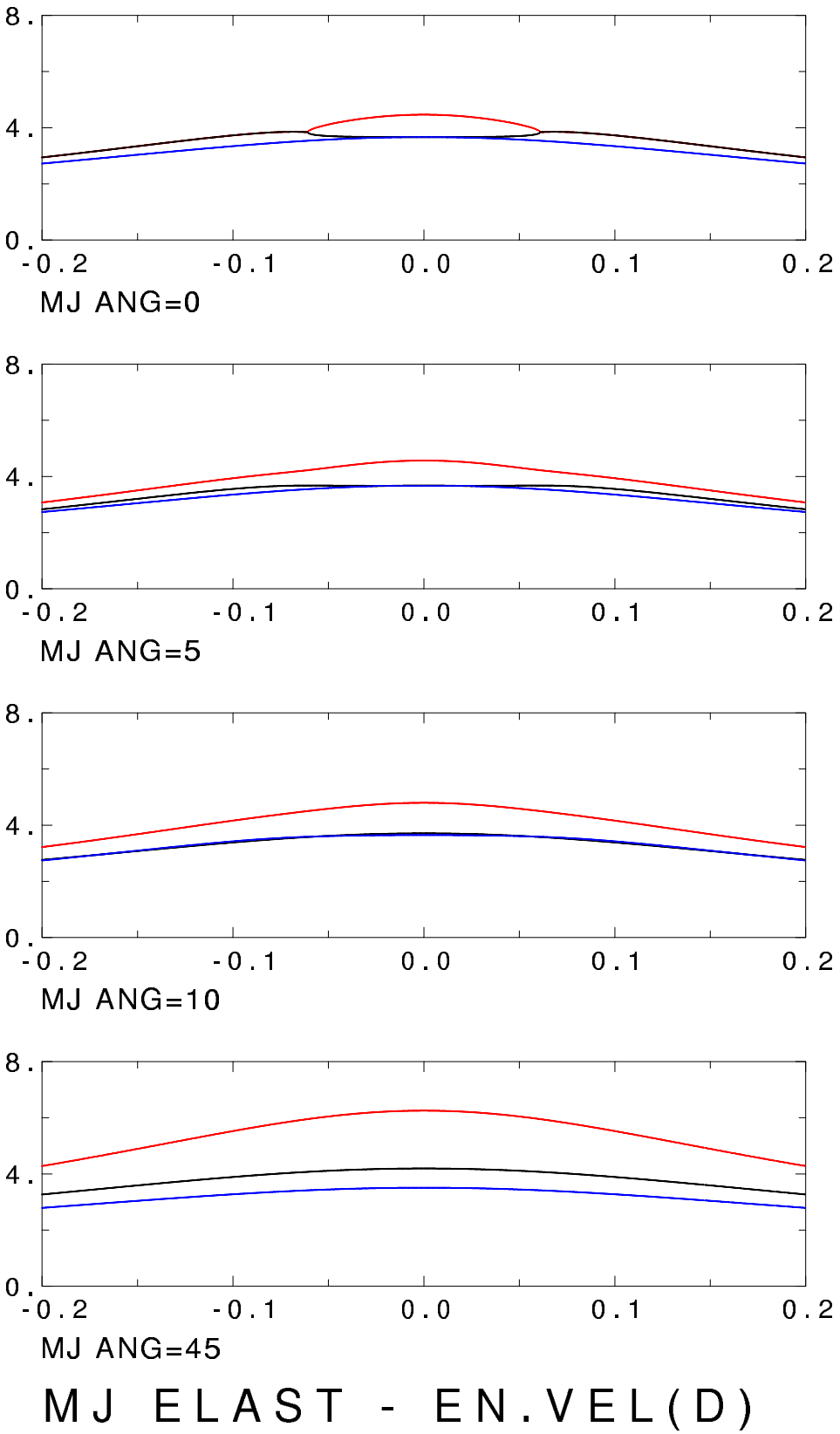
8.
4.
0.
-0.2
-0.1
0.0
0.1
0.2
MJ ANG=0
MJ ANG=5
MJ ANG=10
MJ ANG=45
MJ ELAST - EN.VEL(D)

Figure 10

reaches nearly 20^0. For $i = 5^0$, the plot becomes strongly non-symmetric with respect to $D = 0$. The energy angle of the SH wave is again independent of D, but it differs slightly from zero. From the changing colour with varying D, we can see that for some D the SH wave is slower than the SV wave, for other D, it is faster. The energy angles of P and SV waves are symmetric with respect to the value of the energy angle of the SH wave. For $i = 10^0$, the variation of energy angles of all waves becomes less pronounced, for $i = 45^0$, it is nearly constant.

For comparison, Fig.12 shows the same results but for planes waves propagating in a perfectly elastic anisotropic medium. Except for $i = 0^0$, the plots are again similar to those shown in Fig.11. For $i = 0^0$, the energy angle of the SH wave is again constant and equal zero. The same holds for energy angles of the P and SV waves for $|D|$ less than approximately 0.06. Outside this interval, behaviour of P and SV waves is non-distinguishable, see Fig.10 for $i = 0^0$. Therefore, the curves of P and SV waves are represented by a random combination of red and black points.

The **attenuation-energy angles** of all three waves shown in Fig.13 behave similarly as the same angles of SH waves in Figs.1 and 3. They are always less than 90^0, which distinguishes them from the attenuation angles, see Červený and Pšenčík (2005b), which may be greater or less than 90^0. As in Figs.1 and 3, the attenuation-energy angle becomes zero for D, which is, in most cases, different from $D = 0$. For the propagation angle $i = 0^0$, the attenuation-energy angle is, however, zero for exactly $D = 0$.

We do not show behaviour of attenuation-energy angles of P, SV and SH plane waves for perfectly elastic medium because in that case the attenuation-energy angles are constant and equal to 90^0.

Finally, in Fig.14, we show behaviour of loss factor for the above set of propagation angles. We can see that behaviour of loss factor of P and SV waves is quite different from behaviour of SH waves, see nearly constant curve in Fig.14 or curves in Figs.1 and 3. We can see that except for $i = 45^0$, the P-wave loss factor has pronounced maximum for D close to zero, whereas the SV-wave loss factor has pronounced minimum there. It means that in the directions close to the vertical axis, homogeneous and weakly inhomogeneous P waves will be substantially more dissipated than corresponding SV waves. For $i = 45^0$, the situation changes. Dissipation of SH waves is always small and practically independent of D.

We do not show behaviour of loss factor of P, SV and SH plane waves propagating in a perfectly elastic medium because in that case the loss factors are identically zero.

Acknowledgements

The research has been supported by the Consortium Project "Seismic Waves in Complex 3-D Structures", by the Research Project 205/05/2182 of the Grant Agency of the Czech Republic, and by the Research Project A3012309 of the Grant Agency of the Academy of Sciences of the Czech Republic. Thanks to Morten Jakobsen for providing the data for numerical examples.

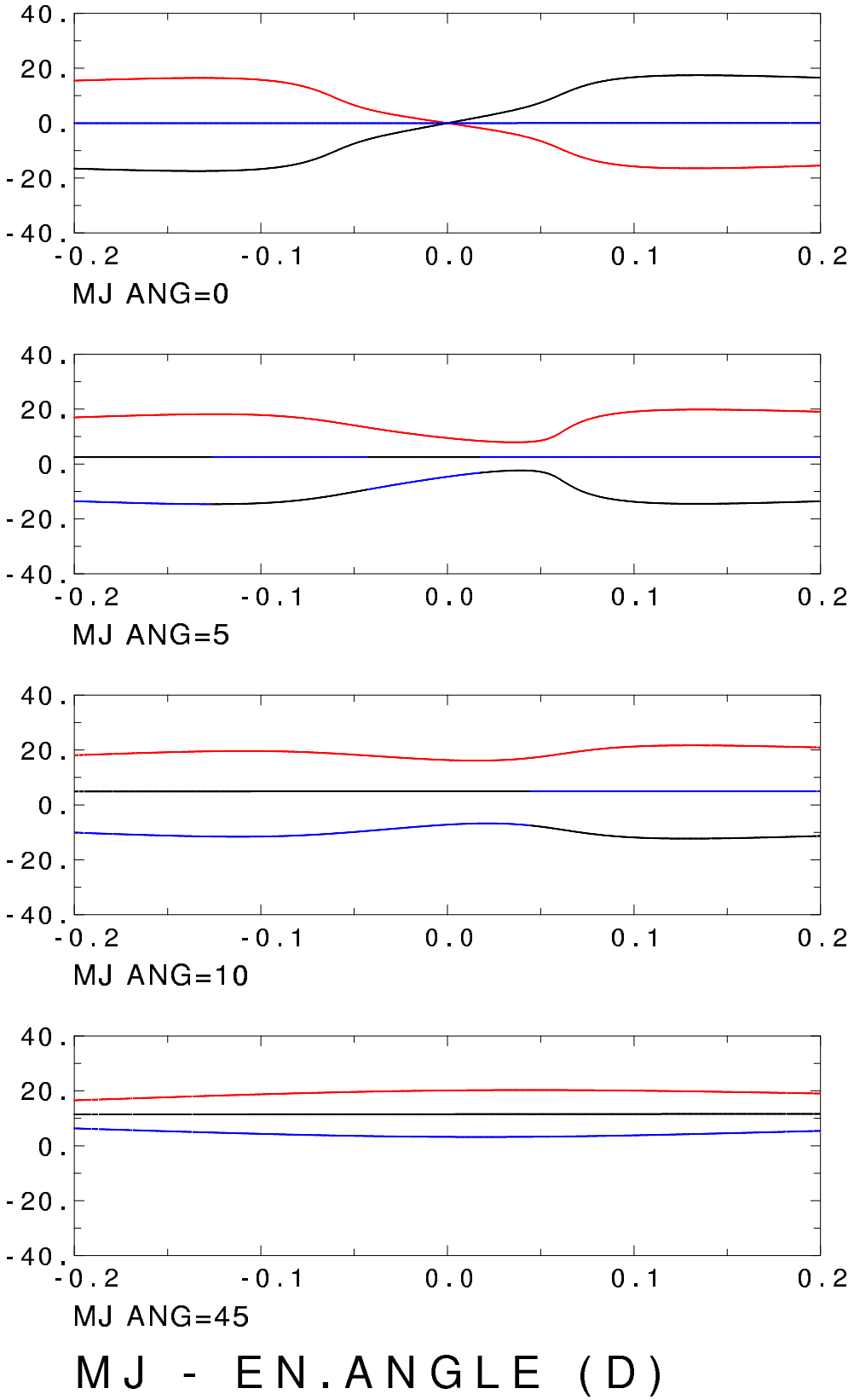
40.
20.
0.
-20.
-40.
-0.2
-0.1
0.0
0.1
0.2
MJ ANG=0
MJ ANG=5
MJ ANG=10
MJ ANG=45
MJ - EN.ANGLE (D)

Figure 11

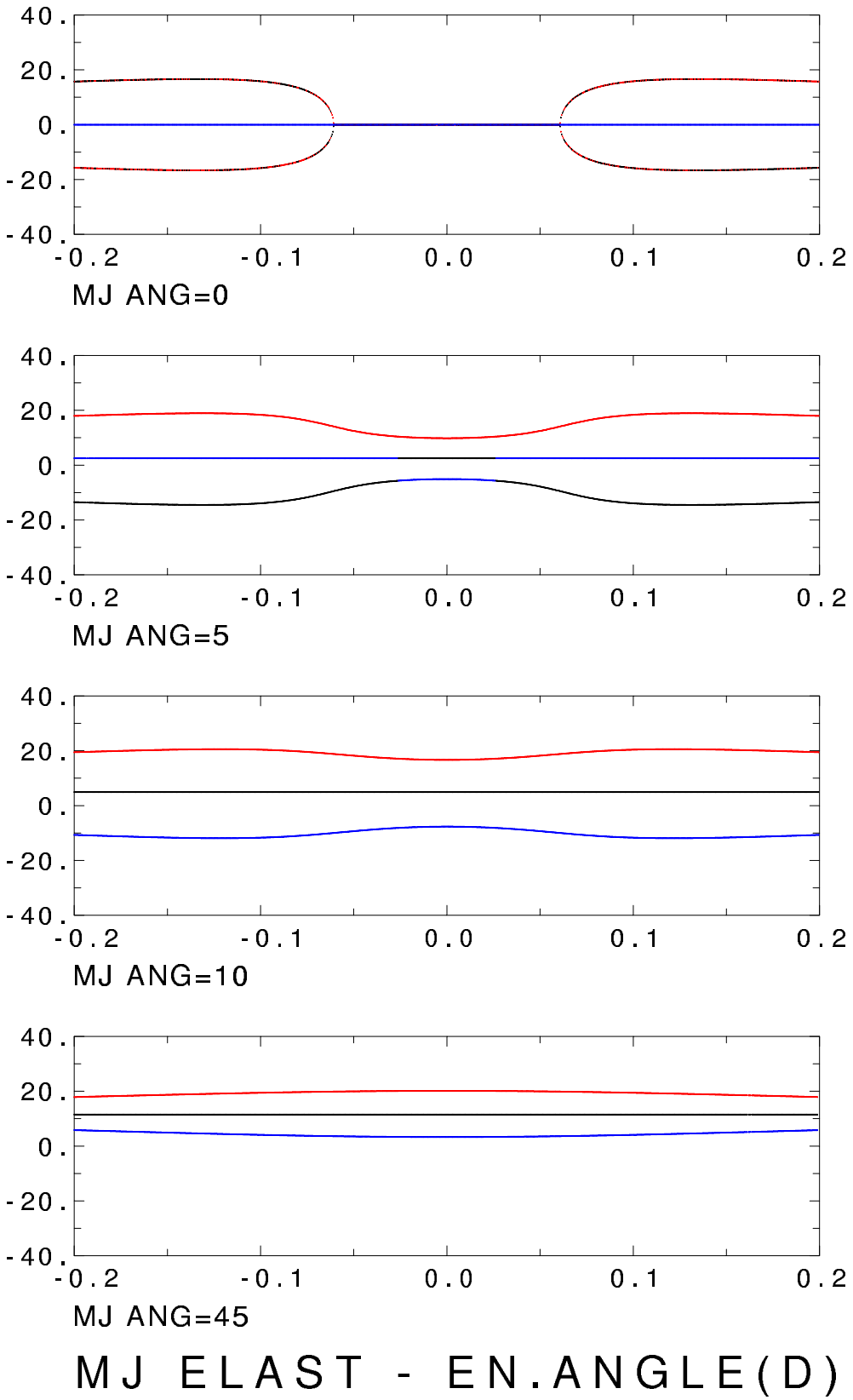
40.
20.
0.
-20.
-40.
-0.2
-0.1
0.0
0.1
0.2
MJ ANG=0
MJ ANG=5
MJ ANG=10
MJ ANG=45
MJ ELAST - EN.ANGLE(D)

Figure 12

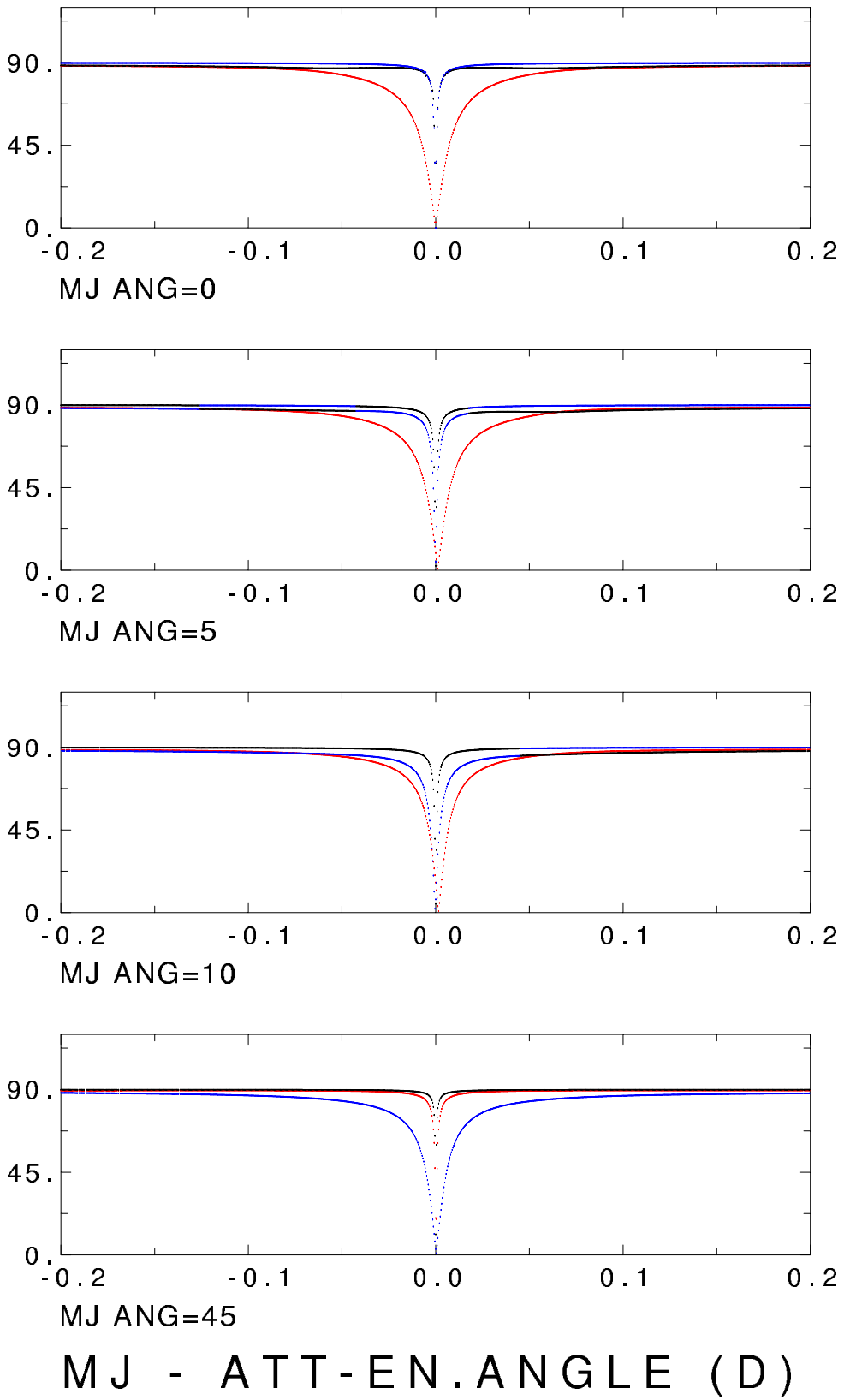
90.
45.
0.
-0.2
-0.1
0.0
0.1
0.2
MJ ANG=0
MJ ANG=5
MJ ANG=10
MJ ANG=45
MJ - ATT-EN.ANGLE (D)

Figure 13

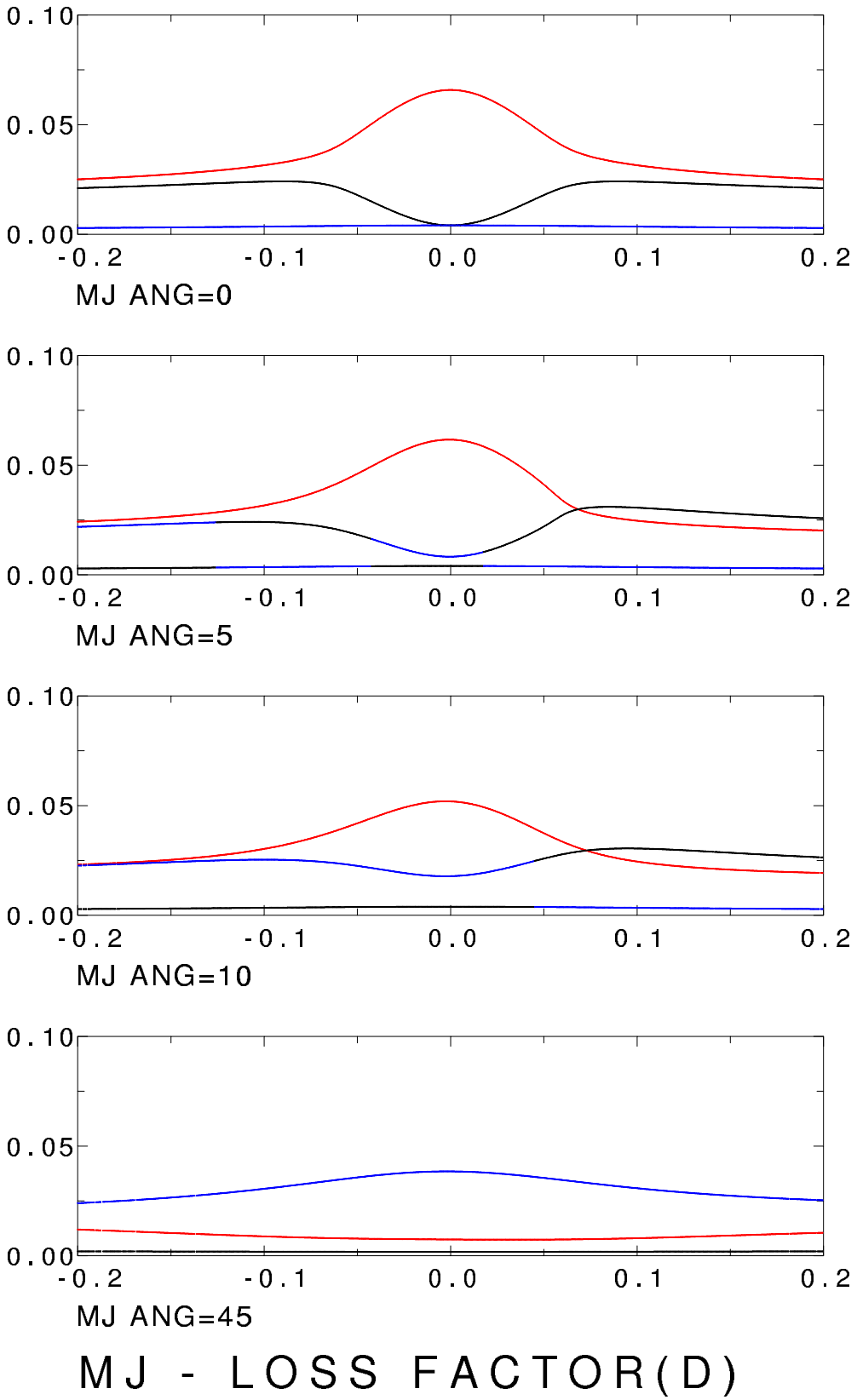
0.10
0.05
0.00
-0.2
-0.1
0.0
0.1
0.2
MJ ANG=0
MJ ANG=5
MJ ANG=10
MJ ANG=45
MJ - LOSS FACTOR(D)

Figure 14

References

Ainslie, M.A., and Burns, P.W. (1995). Energy conserving reflection and transmission coefficients for a solid-solid boundary. *J. acoust. Soc. Am.*, **98**, 2836–2840.

Aki, K., and Richards, P.G. (1980). *Quantitative seismology.* Freeman, San Francisco.

Auld, B.A. (1973). *Acoustic fields and waves in solids.* Wiley, New York.

Borcherdt, R.D. (1973). Energy and plane waves in linear viscoelastic media. *J. Geophys.Res.*, **78**, 2442–2533.

Borcherdt, R.D., and Wennerberg, L. (1985). General P, type-I S and type-II S in anelastic solids: Inhomogeneous wave fields in low-loss solids. *Bull. seism. Soc. Am.*, **75**, 1729–1763.

Brokešová, J., and Červený, V. (1998). Inhomogeneous plane waves in dissipative isotropic and anisotropic media. Reflection transmission coefficients. In *Seismic waves in complex 3-D structures, Report 7*, pp. 57–146. Charles University, Faculty of Mathematics and Physics, Dept. of Geophysics, Praha. (Available online at "http://sw3d.mff.cuni.cz".)

Buchen, P.W. (1971). Plane waves in linear viscoelastic media. *Geophys. J.R. astr. Soc.*, **23**, 531–542.

Burridge, R. (1976). *Some mathematical topics in seismology.* Courant Inst. of Math. Sci., New York Univ., New York.

Carcione, J.M. (1994). Wavefronts in dissipative anisotropic media. *Geophysics*, **59**, 644–657.

Carcione, J.M. (1995). Constitutive model and wave equation for linear, viscoelastic, anisotropic media. *Mech. Mat.*, **19**, 311–327.

Carcione, J.M. (1997a). Reflection and refraction of anti-plane shear waves at a plane boundary between viscoelastic anisotropic media. *Proc. R. Soc. Lond. A*, **453**, 919–942.

Carcione, J.M. (1997b). Reflection and transmission of qP-qS plane waves at a plane boundary between viscoelastic transversely isotropic media. *Geophys. J. Int.*, **129**, 669–680.

Carcione, J.M. (2001). *Wave fields in real media: Wave propagation in anisotropic, anelastic and porous media.* Pergamon, Amsterdam.

Carcione, J.M., and Cavallini, F. (1993). Energy balance and fundamental relations in anisotropic-viscoelastic media. *Wave Motion*, **18**, 11–20.

Carcione, J.M., and Cavallini, F. (1995). Forbidden directions for inhomogeneous pure shear waves in dissipative anisotropic media. *Geophysics*, **60**, 522–530.

Caviglia, G., and Morro, A. (1992). *Inhomogeneous waves in solids and fluids.* World Scientific, Singapore.

Caviglia, G., and Morro, A. (1999). Existence and uniqueness in the reflection-transmission problem. *Q.J. Mech. Appl. Math.*, **52**, 543–564.

Červený, V. (2001a). *Seismic ray theory.* Cambridge Univ. Press, Cambridge.

Červený, V. (2001b). Energy flux of time-harmonic waves in anisotropic dissipative media. In: *Seismic waves in complex 3-D structures, Report 11*, pp. 301–314, Charles University, Faculty of Mathematics and Physics, Dept. of Geophysics, Praha. (Available online at "http://sw3d.mff.cuni.cz".)

Červený, V. (2004). Inhomogeneous harmonic plane waves in viscoelastic anisotropic media. *Stud. Geophys. Geod.*, **48**, 167–186.

Červený, V., and Pšenčík, I. (2005a). Plane waves in viscoelastic anisotropic media. I. Theory. *Geophys. J. Int.*, **161**, 197–212.

Červený, V., and Pšenčík, I. (2005b). Plane waves in viscoelastic anisotropic media II. Numerical examples. *Geophys. J. Int.*, **161**, 213–229..

Deschamps, M. (1990). Réflexion-réfraction de l'onde plane hétérogène: Repartition de l'énergie. *J. Acoust.*, **3**, 251–261.

Deschamps, M., and Poncelet, O. (2002). Inhomogeneous plane wave and the most energetic complex ray. *Ultrasonics*, **40**, 293–296.

Fedorov, F.I. (1968). *Theory of elastic waves in crystals.* Plenum, New York.

Frazer, L.N., and Fryer,, G.J. (1989). Useful properties of the system matrix for a homogeneous anisotropic visco-elastic solid. *Geophys. J.*, **97**, 173–177.

Gajewski, D., and Pšenčík, I. (1991).

Hanyga, A. (1999). Asymptotic theory of wave propagation in viscoporoelastic media. In *Theoretical and Computational Acoustics '97*, eds. Teng, Y.-C., Shang, E.-C., Pao Y.-H., Schulz, M.H. and Pierce, A.D., pp. 429–448. World Scientific, Singapore.

Hanyga, A., and Seredyńska, M. (1999). Thermodynamics and asymptotic theory of wave propagation in viscoporous media. In *Theoretical and Computational Acoustics*, **97**, eds. Teng, Y.-C., Shang, E.-C., Pao Y.-H., Schulz, M.H. and Pierce, A.D., pp. 449–456. World Scientific, Singapore.

Hayes, M. (1980). Energy flux for trains of inhomogeneous plane waves. *Proc. R. Soc. Lond. A*, **370**, 417–429.

Helbig, K. (1994). *Foundations of anisotropy for exploration seismics.* Pergamon, Oxford.

Jakobsen,M., Johansen,T.A. & McCann,C., 2003. The acoustic signature of fluid flow in complex porous media. *J.Appl.Geophys.* **54**, 219–246.

Krebes, E.S. (1983). Discrepancies in energy calculations for inhomogeneous waves. *Geophys. J.R. astr. Soc.*, **75**, 839–846.

Krebes, E.S., and Le, L.H.T. (1994). Inhomogeneous plane waves and cylindrical waves in anisotropic anelastic media. *J. Geophys. Res.*, **99**, No. B12, 23899–23919.

Leroy, O., Quentin, G., and Clayes, J.M. (1988). Energy conservation for inhomogeneous plane waves. *J. acoust. Soc. Am.*, **84**, 374–378.

Mann, J.A., Tichy, I., and Romano, A.J. (1987). Instantaneous and time-averaged energy transfer in acoustic fields. *J. acoust. Soc. Am.*, **82**, 17–29.

Richards, P. (1984). On wavefronts and interfaces in anelastic media. *Bull. seismol. Soc. Am.*, **74**, 2157–2165.

Shuvalov, A.L. (2001). On the theory of plane inhomogeneous waves in anisotropic elastic media. *Wave Motion*, **34**, 401–429.

Shuvalov, A.L., and Scott, N.H. (1999). On the properties of homogeneous viscoelastic waves. *Q.J. Mech. Appl. Math.*, **52**, 405–417.

Shuvalov, A.L., and Scott, N.H. (2000). On singular features of acoustic wave propagation in weakly dissipative anisotropic thermoviscoelasticity. *Acta Mechanica*, **140**, 1–15.

Thomson, C.J. (1996a). *Notes on Rmatrix, a program to find the seismic plane-wave response of a stack of anisotropic layers.* Queen's University, Dept. of Geol. Sci., Kingston.

Thomson, C.J. (1996b). *Notes on waves in layered media to accompany program Rmatrix.* Queen's Univ., Dept. of Geol. Sci., Kingston.